# Phototrophic microbial fuel cells for sustainable power generation and wastewater treatment

Jayesh M. Sonawane[a,b*], Ankisha Vijay[d], Tianyang Deng[b], Prakash C. Ghosh[d], Jesse Greener[b,c*]

[a*]Department of Chemical Engineering & Applied Chemistry and Centre for Global Engineering, University of Toronto, Canada M5S 3E5

[b]Département de Chimie, Faculté des sciences et de génie, Université Laval, Québec City, QC, Canada

[c]CHU de Québec, Centre de recherche, Université Laval, 10 rue de l'Espinay, Québec, QC, Canada

[d]Department of Energy Science and Engineering, Indian Institute of Technology Bombay, Mumbai, India. 400 076

[e]Department of Biotechnology, Jaypee Institute of Information Technology, Noida, Uttar Pradesh, 201307, India

[*]Corresponding author –
Jayesh M. Sonawane - jay1iisc@gmail.com; jayesh.sonawane.1@ulaval.ca
Jesse Greener - jesse.greener@chm.ulaval.ca

## Abstract

Microbial fuel cells (MFCs) rely on the capacity of electrode-adhered electroactive bacteria to oxidize organic matter and generate electrons. Typical MFCs are highly engineered systems that can be applied as green tools to alleviate the burden of waste streams. Phototrophic MFCs (PhMFCs) are a promising variant that can be implemented indoors or outdoors and use the power of the sun to boost efforts in on-site environmental remediation, biomass generation, and power generation. PhMFC variations include plant-based and algal-based MFCs. Algal-based MFCs can incorporate special photosynthetic action at either the anode or electrode, enhancing or replacing the role of other bacteria in regular bacterial MFCs. Plant-based MFCs

can be more complex due to the role of the root system near an electrode and its interaction with electrode-adhered bacteria, and they are nearly universally operated outdoors in either natural or engineered conditions. This review considers PhMFCs such as algal-based MFCs, algal carbon capture cells (ACCCs) and anode algal microbial fuel cells (AAMFCs), and also plant-based MFCs which include natural plant MFCs (NPMFCs), constructed wetland MFCs (CWMFCs), and marine-rooted plant MFCs (MPMFCs). After summaries of the fabrication and function of different PhMFCs, we elaborate with a literature review and discussion on each variant, followed by suggestions for future directions that will enhance the impact and accelerate the uptake of these promising multi-functional biosystems.

**Keywords:** Natural plant microbial fuel cells, algae-MFC, rhizodeposits, constructed wetland MFC, wastewater treatment, power production.

**Highlights**

- Generation of green bioelectricity with plant-based MFCs (PMFCs)
- Determination of efficient plants and crops for PMFCs
- Critical review of PMFC configurations and applications such as pollutant removal and biosensing

**Abbreviations and common terms**

| | |
|---|---|
| AC | Activated carbon |
| ACCC | Algal carbon capture cell |
| AAMFC | Anode algal microbial fuel cell |
| BER | Biofilm electrode reactor |
| CE | Coulombic efficiency |
| COD | Chemical oxygen demand |
| CW | Constructed wetlands |
| CWMFC | Constructed wetland microbial fuel cell |
| DO | Dissolved oxygen |
| EAB | Electroactive bacteria |
| HRT | Hydraulic retention time |
| MFC | Microbial fuel cell |

| | |
|---|---|
| MPMFC | Marine-rooted plant microbial fuel cell |
| NPMFC | Natural-plant microbial fuel cell |
| $P_A$ | Power normalized by anode area |
| PAC | Powdered activated carbon |
| PEM | Proton exchange membrane |
| PhMFC | Phototrophic microbial fuel cell |

## 1.1 Introduction

Freshwater aquatic life faces threats due to pollution from pesticides, pharmaceuticals, heavy metals, and herbicides, all of which find can their way into natural waterways [1,2]. In response, demands are growing for real-time water quality monitoring and new methods for remediating polluted environmental sites [3,4]. At the same time, the continued use of fossil fuels, which has pushed $CO_2$ levels from 388.5 ppm in 2009 to 421 ppm in 2022 [5], underscores the urgent need for alternative solutions based on renewable sources such as solar and biomass.

The typical microbial fuel cell (MFCs) is a promising green technology that uses heterotrophic electroactive biofilms (EABs) to produce energy by degrading organic compounds, including polluting substances [6–9]. The chemical energy present in such compounds is converted into electricity by a redox process that couples to the metabolic pathway of microorganisms present in the EAB [4,10,11]. The components of the MFC include an anode and cathode separated by a proton exchange membrane (PEM). Typically, the anode-adhered EAB oxidizes dissolved organic compounds and transfers electrons into the external circuit. From there, electrons perform work across an electrical load before arriving at the cathode, where electron acceptors are reduced and complete the redox cycle [12,13]. The performances of all types of MFC devices are characterized by certain figures of merit, which include substrate conversion rates, conversion efficiency, electrode overpotential, membrane transport properties, internal resistance, and power output.

Noteworthy factors that affect these figures of merit are bacterial species, solution pH, temperature, electrode materials, electrode surface area, concentration of biological oxygen demand, and chemical oxygen demand (COD) [14]. The two most important figures of merit are power density (Eqn. 1) and conversion efficiency (Eqn. 2):

$$P_A = V^2/R_{ext}A \hspace{5cm} \text{(Eqn. 1)}$$

where $P_A$ is the areal normalized power density, V is the measured cell potential, $R_{ext}$ is the external resistance, and A is the projected area of the electrode (anode). Coulombic efficiency ($\eta_C$) is defined as the ratio of the total amount of charge generated from organic molecule substrate molecules that is transferred to the MFC external circuit to the theoretical maximum charge that can be generated from these molecules [15–17].

$$CE = \frac{MQ}{F \cdot n \cdot V \cdot COD_{EF}} \cdot 100 \qquad \text{(Eqn. 2)}$$

where M is the molecular weight of oxygen (32 g mol$^{-1}$), Q is the total charge collected from substrate oxidation (C), F is Faraday`s constant (C mol$^{-1}$), n is the number of electrons exchanged per mole of oxygen (4), V is the volume of the anode chamber (L), and $COD_{EF}$ is the percent cumulative COD removal efficiency (%). We note that COD is often used as a convenient measure of substrate concentration.

MFC variants have proliferated, including those that incorporate photosynthetic elements such as plants and algae, which are classified as phototrophic MFCs (PhMFCs) [18,19] (Figure 1). In these devices, electroactive and photosynthetic organisms work symbiotically to generate and enhance MFC performance. A typical figure of merit for PhMFCs quantifies the efficiency in electron production based on the local light intensity (Eqn. 3).

$$\Phi_A = I/F_p \qquad \text{(Eqn. 3)}$$

where $\Phi_A$ is the apparent quantum yield, which is based on the ratio between the current (I) and $F_p$, the average photon flux [20]. Phototrophic MFCs are further classified as natural plant MFCs (NPMFCs), constructed wetland MFCs (CWMFCs), and marine-rooted plant MFCs (MPMFCs). Algae-based MFCs are further classified as anode algal MFCs (AAMFCs), in which the photosynthetic process at the anode helps produce power, and algal carbon capture cells (ACCC), in which algae at the cathode chamber transform $CO_2$ by-products from the anode into biomass with the aid of energy from absorbed photons. The classification of PhMFCs is illustrated in Figure 1. We note that the vast majority of PhMFC papers deal with systems with distinct plant or algal phototrophs. However, while there exists some work in which both types of phototrophs are used in the same device [21,22], they are not reviewed here.
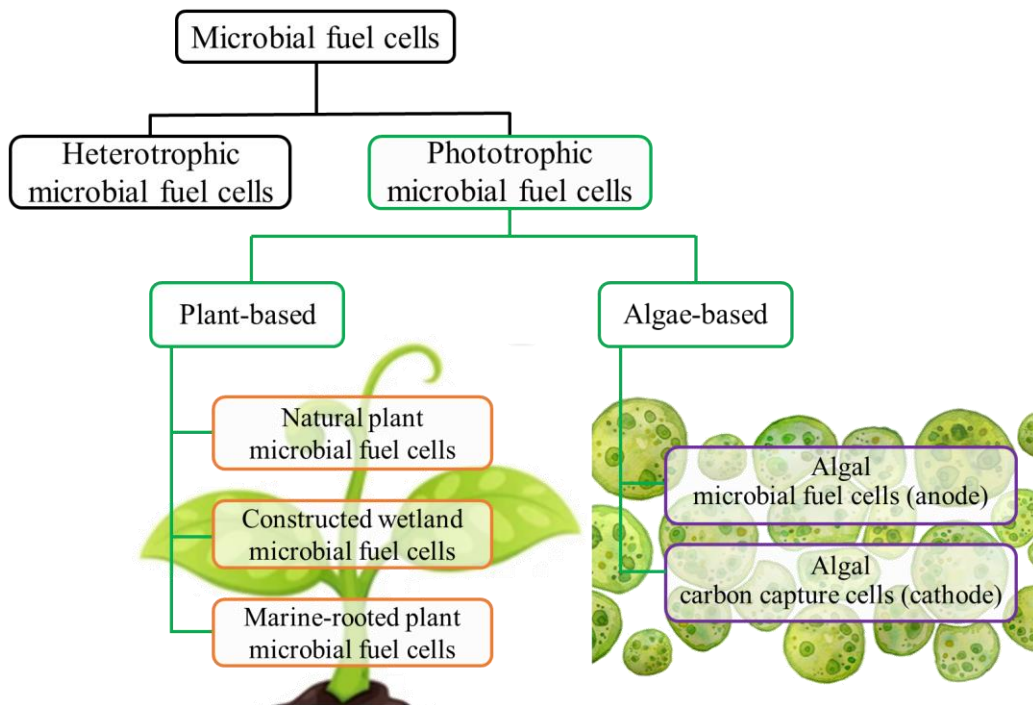
**Figure 1.** Classification of phototrophic microbial fuel cells (PhMFC). PhMFCs are classified based on use of plants and algae for power generation.

## 1.2 Plant and algae primer

Plants are complex photosynthetic organisms that localize photosynthesis largely in their leaves. They also possess a complex root system that provides anchorage, water absorption, and nutrition. The root system is protected from harmful bacteria and fungi by secretions that form a gelatinous polysaccharide layer that coats the root segments. Root secretions into the surrounding soil (called rhizodeposits) also include proteins, enzymes, amino acids, DNA, and sugars. Together these components help to create a niche in which the roots and supporting microorganisms can thrive. Different plant-based MFCs exist, but all involve the interaction of the root system with the anode, primarily through the symbiotic relationship between electrode-adhered electroactive bacteria and the plant root rhizodeposits.

The other major class of phototrophs is algae. Algae are a highly varied class of aquatic photosynthetic microorganisms and their clusters, which can also inhabit hydrated soils and other complex matrices. Algae vary in size and life cycle and especially in photosynthetic pigments and other cellular features, more so than plants. Algae (eukaryotes) differ from cyanobacteria (prokaryotes) in that they contain nuclei, and they lack the reproductive structure, roots, leaves, and stem systems of plants. Similar to cyanobacteria and plants, algae contain the apparatus for photosynthesis. Early classification of algae was based on their

characteristic color (e.g., green, red, and brown), which is derived from different light-absorbing (chloroplast) pigments, including chlorophylls (a and b), phycobiliproteins (which largely absorb blue or red light), and carotenoids (which largely absorb blue and green light). These definitions resulted in the consideration of cyanobacteria as algae, even though the two microbes are fundamentally different. As there is much overlap in naming of photosynthetic microorganism species, some references may also be made to plankton (including picoplankton), which are a mix of algae and bacteria including photosynthetic variants. For the sake of simplicity, however, we do not differentiate between different photosynthetic microorganisms, when discussing algal-based MFCs.

Apart from their historic and ongoing planetary importance in oxygen production, which is responsible for 75% of global oxygen [23], algae are the traditional sources of crude oil and food sources and form the basis of new markets related to pharmaceuticals and other industrial products. Engineered photobioreactors are rapidly advancing towards closed, illuminated systems in which physical and chemical parameters can be highly tuned to maximize the growth of algal biomass with minimal cost [24,25]. In the context of the current application, algae (and cyanobacteria) are also emerging as critical components in both natural environment and engineered PhMFCs. Specific to their role in enhancing MFC performance, algae can efficiently produce carbohydrates, lipids, proteins, and pigments and absorb $CO_2$, which can aid the growth of anode-adhered electroactive bacteria. Algae can also produce $O_2$ to enhance oxygen reduction at the cathode.

In either plant-based or algal photosynthesis, the overall reaction of photosynthesis and its Gibbs free energy change per mole of glucose produced are shown in Eqn. 4.

$$6CO_2 + 6H_2O \xrightarrow{\text{light}} C_6H_{12}O_6 + 6O_2, \Delta G^0 = 2872 \text{ kJ/mol} \qquad \text{(Eqn. 4)}$$
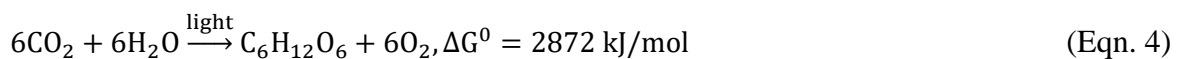
Once photons are captured by the pigment, they are transferred to photosystems (PS) that are embedded in the intracellular thylakoid membrane within the cytoplasm. Universally, there are two types of photosystems, PSI and PSII, which work synergistically. First, water is split at PSII by a charge separation step, which activates a manganese-based catalysis to separate protons and molecular oxygen. This process can be simplified as shown in Eqn. 5, along with the potential (V) based on the per mol Gibbs free energies involved.

$$2H_2O \rightarrow \frac{1}{2}O_2 + 2H^+ + 2e^-, \Delta\varepsilon^0 = 0.81\ V \hspace{2cm} \text{(Eqn. 5)}$$

Electrons are transferred via heme-containing proteins (cytochromes, such as the membrane-bound Cyt $b_6f$) to PSI, where the process of converting $NADP^+$ to NADPH begins. A proton flux to the enzyme ATP-synthase (ATP-ase) drives the conversion of ADP to ATP. Finally, NADP, ATP, and $CO_2$ are integrated into the Calvin-Benson-Bassham cycle (Calvin cycle) to produce polysaccharides. These steps are summarized in Figure 2.
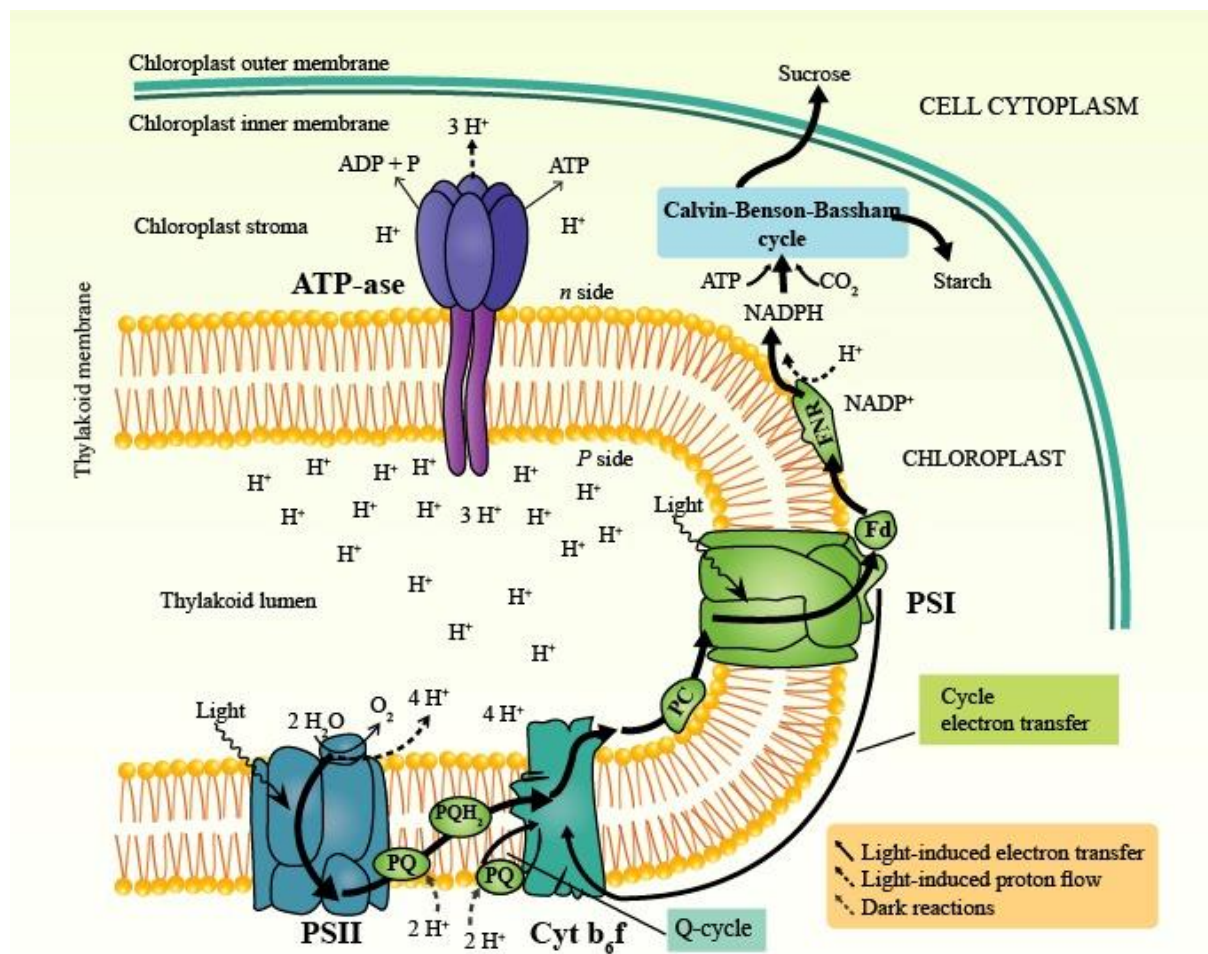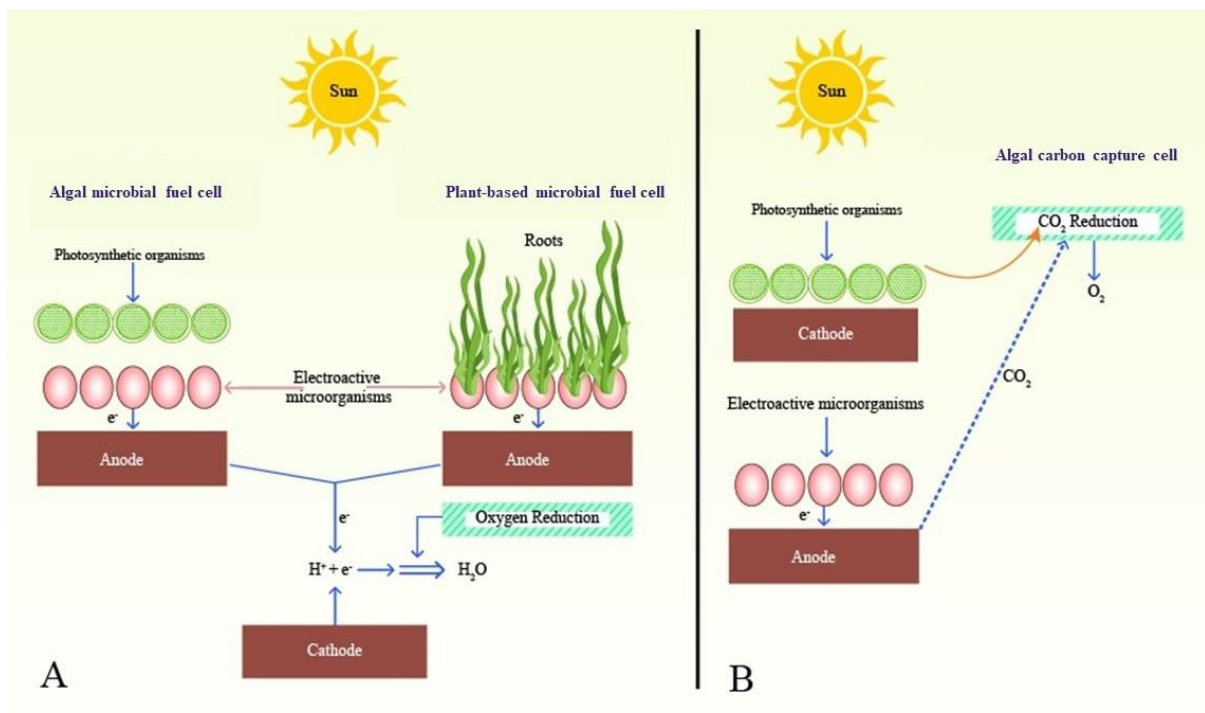


**Figure 2.** Schematic representation of the photosynthetic processes occurring in plant and algal thylakoid membranes and the protein complexes involved. Adapted from previous work [26].

## 1.3 Role of plants and algae in different phototropic microbial fuel cells

The process by which solar energy is absorbed and by which organic matter is transported within the PhMFC is used as a means for categorization. There are four major mechanisms involved in all PhMFCs, namely, (1) photosynthesis, (2) mass transport of organic compounds to the anode compartment, (3) oxidation of organic matter though the metabolism of the EAB

and through that of other anode-chamber consortia members, and (4) bioelectrochemical reduction reactions at the cathode, including oxygen reduction. This is illustrated in Figure 3 [27], which demonstrates fundamental differences between anode supporting PhMFCs (all plant-based MFC (NPMFC, CWMFC, MPMFC) and AAMFCs) and ACCC MFCs. The process of photosynthesis in plants uses solar energy to fix carbon dioxide in the form of carbohydrates. In regards to plant-based MFCs, as much as 60% of the fixed carbon can be moved to plant roots depending on the MFC variant, plant age, species, and environmental conditions [28].



**Figure 3.** Schematic representation of different PhMFCs, including those in which photosynthetic elements (a) interact with the anode (algal MFCs and plant-based MFCs) and (b) interact with the cathode (algal carbon capture cells). Figure adapted from a previous study [27].

Further information about each PhMFC variant is given in Table 1, including the primary role, location of each electrode, and common substrates. For example, in addition to producing power, some PhMFC aid in the remediation of contaminated waste streams (CWMFC), while others (ACCC) can produce different useful compounds such as ethanol, hydrogen, methane, and $H_2O_2$ [29]. In AAMFCs, some of the by-products or the algae themselves can be useful as substrates for electroactive bacteria [30–32].

**Table 1.** Various types of phototrophic microbial fuel cells

| MFC variations | Anode position | Cathode position | Substrates | Function(s) |
|---|---|---|---|---|
| Natural plant (NPMFC) | Area surrounding the rhizosphere | Soil-water interface | Rhizodeposits from plants | Bioelectricity from plants |
| Constructed wetland (CWMFC) | Aquatic rhizosphere | Area in water | Contaminants in wastewater | Wastewater treatment |
| Marine-rooted plant (MPMFC) | Sediment | Area in water | Natural organic sediment | Bioelectricity and wastewater treatment |
| Anode algal MFC (AAMFC) | Habitat for electrogenic microalgae | Inoculating cathode with algae | Algae biomass and by-products | Bioelectricity and wastewater treatment |
| Algal carbon capture (ACCC) | Habitat for any bioanode producing $CO_2$ | Photosynthetic algae, bacteria | Organic matter | $CO_2$ fixation into by-products |

This review discusses the most recent 5 years of progress in and applications of phototrophic MFCs (PhMFCs) related to plants and algae, with a focus on plant-based systems. First, we describe the working mechanism and factors related to the performance of plant-based and algal-based MFCs. Second, we critically discuss the application of PhMFC devices and indicate the existing gaps. Finally, we assess future perspectives associated with these devices.

## 2. Plant-based microbial fuel cell

In all plant-based MFCs, electrodes are found in a natural earthen matrix (soil or benthic sediment), where electroactive bacteria produce electrons. This contrasts with soil, and benthic

MFC, where the earthen matrix material serves as the sole source of inoculum and nutrients for anode-adhered EABs, and nutrients supplied to the anode-adhered EAB in plant-based MFCs are supplemented by root exudates (fluids emitted through the plant roots) [33–38] and related dead cell material. In addition to having a high availability of substrate molecules, the anode chamber should also be free of electron acceptors such as nitrate, $CO_2$, and oxygen. Similarities between plant-based MFCs and soil or benthic MFCs are found in the mechanism of electron production, transport and organic removal [39–41]. Plant roots play a critical role in plant-based MFCs by producing various organic compounds, carbon dioxide, ethylene, enzymes, carbohydrates, organic acids, sugars, and dead cell materials [42]. The process of plant-root release is called rhizodeposition, and the products are known as rhizodeposits, accounting for approximately 40% of the productivity due to photosynthesis [43]. Rhizodeposition is present throughout the root environment but is most pronounced at the root tips [44]. Thus, the nutrient support from plant roots in plant-based MFCs consists of by products from photosynthesis [45].

In addition to feeding EABs, carbon sources presented in the rhizodeposits are also used by other microorganisms, which help to maintain and protect the plant roots and potentially the EAB. The combination of nutrient support and maintenance of healthy culture conditions has been shown to increase the activity of the microbes present in the soil near the root of a plant by nearly a factor of 10 [46]. Plant-based MFCs serve a similar role as other MFCs and are able to remediate plant root environments (soil, sediment) while providing energy, but they distinguish themselves by also supporting the growth of plant biomass and $CO_2$ conversion to $O_2$. It should be noted, of course, that $CO_2$ fixation is followed by $CO_2$ emissions at the bioanode during EAB conversion of nutrients, including those from rhizodeposits. The productivity of any of these roles depends on the efficiency of key processes. Thus, the advantages and drawbacks should be evaluated and compared with other methods along the lines of energy efficiency, degree and rapidity of environmental remediation, and economic viability.

Because plant-based MFCs obtain substrate molecules from photosynthesis, the supply of exogenous nutrients or organic elements from sources other than the plant roots can be avoided [47]. The production of oxygen and fixation of $CO_2$ by the plants for photosynthesis can be divided into three categories based on photosynthesis conditions, namely, plants carrying out photosynthesis with ideal temperatures of 15–25°C (C3), tropical plants carrying out photosynthesis with ideal temperatures of 30–40°C (C4), and plants carrying out

photosynthesis in semi-dry climatic conditions with ideal temperatures greater than 40°C (CAM) [48]. The highest levels of photosynthetic activity and rhizodeposition are exhibited by plants belonging to the C4 category due to the combined benefit of well-hydrated environments and improved metabolic activity due to elevated temperatures [49].

Among the plant-based MFC subclasses is the natural-plant MFC (NPMFC). This variant has emerged as a promising technology in green roofs, reactive barriers, and environmental biosensors. Although NPMFCs were originally developed for the production of bioenergy from the rhizodeposits, [50] they have also been demonstrated for wastewater treatment, food production by utilization of waste organic material, and degradation of starch and biocathode autotrophic denitrification [51–53]. The EAB metabolism in NPMFCs is directly related to current generation [54,55], which indicates that there are no secondary processes related to plant-roots that contribute directly to electrical outputs. Because EAB metabolisms are sensitive to the presence of different bioactive compounds, changes in current are the basis of MFC environmental sensors [56]. Similarly, a self-powered NPMFC architecture was designed with a wireless-based sensor network to analyze the environment. The NPMFC was designed using the *Sansevieria asparagaceae* plant, which generated a stable voltage such that DC current was harvested for the sensor network [57]. The sensors monitored ozone and $CO_2$ via a combination of the NPMFC with EH. A tubular NPMFC designed in a paddy field generated continuous bioelectricity and improved the health of the plants [58]. The most abundant microbes were *Proteobacteria, Verrucomicrobia, Planctomycetes,* and *Acidobacteria.* However, there was no current production during the low rainfall season. Data acquisition was conducted through a LoRa data logger, which offers a prospective use in environmental monitoring. NPMFC was demonstrated for heavy metal detection under light and dark conditions by combining a CuO/ZnO photocathode with an electroactive anode. The developed sensor showed a wide detection range for $Cd^{2+}$ and $Cu^{2+}$ (0.1–4 mg $L^{-1}$ of $Cd^{2+}$ and 10–80 mg $L^{-1}$ of $Cu^{2+}$). The sensor sensitivity was mainly attributed to the intimate P–N heterojunctions formed in the CuO/ZnO [59].

An example schematic of a NPMFC is shown in Figure 4. In this work, three separate NPMFCs were constructed with different plants: fenugreek (*Trigonella foenum-graecum*), mustard (*Brassica juncea*), and a decorative plant (*Canna Stuttgart*). A carbon brush anode that could support microorganisms in the EAB was planted beneath the roots, with the electrical lead emerging from the soil into the air, where a connection was made to a multi-meter. The entire

anode environment was encased in a novel clay separator that could exchange ions and limit electron acceptors from contaminating the anode compartment. The cathode was formed from hydrated carbon cloth around the clay separator, which was otherwise exposed to air. The highest voltage was obtained with *Canna Stuttgart* due to its tuberous roots, which produced large quantities of exudates depending on the amount of organic matter available for the microorganisms. The highest diurnal variation was observed with *Brassica juncea*, based on the lower quantities of root exudates. In contrast, the lowest diurnal variation was shown by *Canna Stuttgart.*[60] Although power generation was stable for all three plants, the highest power density was produced by *Canna Stuttgart* because the exudates from the plant were easily degraded by the microorganisms, resulting in faster oxidation kinetics, higher voltage, and efficient electron donation [60]. A summary of NPMFCs — including various types of plants used, anode and cathode type, type of substrate, and power production from the system, is given in Table 2.

A comparative study that evaluated the performance of stainless steel mesh and graphite-rod anode material in NPMFCs was conducted using two sets of systems. The plant *Vigna radiate Wilzeck* was common to both NPMFCs. The NPMFC with the stainless steel exhibited better performance based on its lower internal resistance [61], but contributions from electrode corrosion should be ruled out. Plant growth was better in the NPMFCs, which was attributed to the accelerated accumulation of photosynthetic products due to the improved metabolic process of the plants [40]. Another set of two NPMFCs was designed using the plant *S. anglica* along with marine sediment and activated carbon as the bioanodes in each case. Although each NPMFC exhibited a considerable power output, the efficiency of the NPMFC was optimal with 33% activated carbon [62]. Furthermore, the presence of marine sediment and activated carbon promoted the growth of the plants, but the growth was lower in the NPMFC with the activated carbon bioanode. Although the microbes present in the activated carbon and marine sediment were different, the most prominent bacteria in the soil were *Proteobacteria*. The results demonstrated that the mixture of marine sediment and activated carbon was suitable for bioanodes, instead of pristine marine sediment bioanodes or activated carbon bioanodes, for effective performance of the NPMFC.
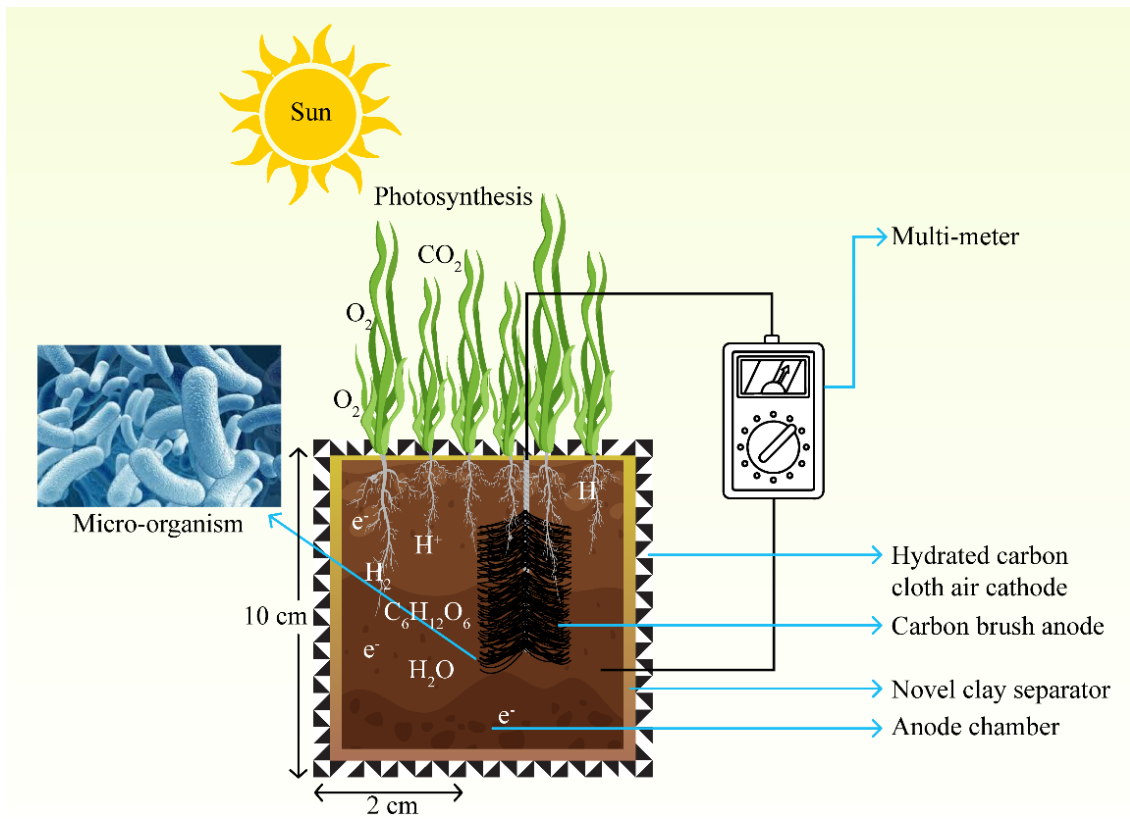
**Figure 4.** Schematic representation of the natural-plant microbial fuel cell system and working principle; figure adapted from a previous study [60].

**Table 2.** Summary of selected studies on NPMFCs, including different types of plants used, anode and cathode type, type of substrate, and power production from the system.

| Plant types | Anode | Cathode | $COD_{EF}$/ VFA/Cr removal (%) | Substrate/Nutrient Solution | $P_A$ (mW m$^{-2}$) | Ref. |
|---|---|---|---|---|---|---|
| *G. maxima* | Graphite granules | Graphite felt | NA | Hoagland medium | 80 | [63] |
| *G. maxima* | Graphite granules | Graphite felt | NA | Hoagland medium | 67 | [64] |
| *E. crassieps* | Graphite discs | Graphite discs | 87 ($COD_{EF}$) 72 (VFA) | Domestic and fermented distillery wastewater | 225 | [65] |
| *L. perenne* | Graphite granules | Carbon felt | 99 [Cr(VI)] | Hoagland medium with sodium acetate | 55 | [66] |
| *S. anglica* | Graphite rod in graphite grains | Graphite felt | NA | Hoagland medium | 222 | [35] |
| *O. sativa* | Graphite granules | Graphite granules | NA | Hoagland solution | 33 | [67] |
| *P. setaceum* | Graphite plate | Graphite plate | NA | Red soil | 163 | [68] |

| | | | | | | |
|---|---|---|---|---|---|---|
| *O. sativa* | Graphite felt | Carbon/polytetrafluorethylene coated | NA | Acetate/glucose, Bacto yeast, electrolyte solution | 19 | [69] |
| *O. sativa* | Graphite granules | Graphite felt | NA | Vermiculite with Hoagland solution | 72 | [70] |
| *S. anglica* | Graphite granules | Graphite felt | NA | Modified Hoagland solution buffered with phosphate buffer | 100 | [71] |

## 3 Constructed wetland microbial fuel cells

CWMFCs are a type of plant-based MFC, but in the CWMFC, flow is controlled so that organic matter from wastewater is spread evenly among the wetland plants. The anode and a cathode in a CWMFC are separated by fibrous materials, soil area, or PEM, as shown in Figure 5.
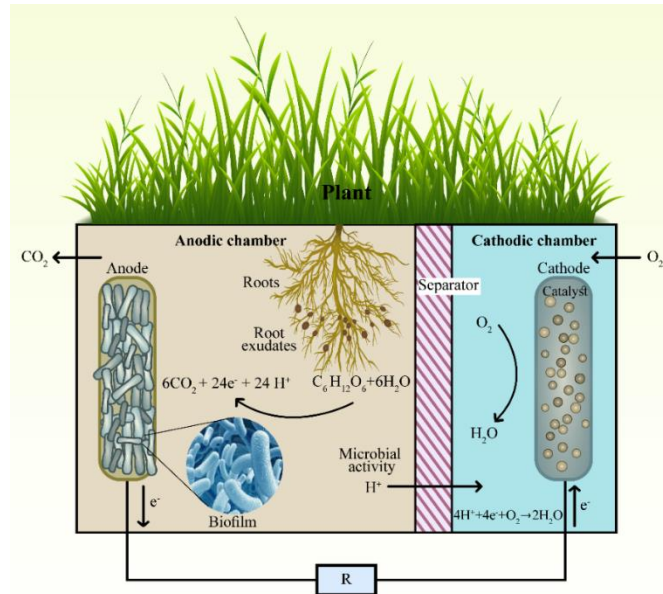


**Figure 5.** Working principle and basic setup for a constructed wetland-microbial fuel cell (CWMFC); figure adapted from a previous study [72].

The biosystem of the CWMFC is categorized as bioprocess and biocontrol. The microbial community is part of the bioprocess, which generates energy from the exudates at the roots. The plant acts as the biocontrol, which absorbs sunlight for transformation into current [40]. Both environmental factors and operating parameters such as temperature, humidity, organic loading, hydraulic retention time (HRT), and redox condition influence the activity of the CWMFC devices. Different aquatic plants can be used, and the primary advantage of the device is production of bioelectricity from natural water without the requirement of external organic substrates, thus lowering the production of methane.

A study was conducted on a CWMFC using dried alum sludge from wastewater treatment plants and powdered activated carbon (PAC) to modify the area around the anode for production of electricity during the treatment of swine wastewater [73]. COD removal and denitrification were increased due to the formation of a denitrification biocathode [74] and electrical stimulation [75]. The COD removal efficiency was 70% for the control system devoid of PAC modification. In comparison, the system with 10% PAC modification exhibited an enhanced COD removal of 80%, which was attributed to the absorption capability of PAC [74].

Reactive phosphate was also efficiently removed thanks to adsorption between phosphorus in the influent and aluminum in the dewatered alum sludge, primarily through ligand exchange and adsorption by PAC [76]. Total nitrogen was decreased due to the presence of aerobic denitrifiers, which used oxygen or nitrate as terminal electron acceptors [77]. The nitrogen in ammonia and total nitrogen was removed due to adsorption by PAC. The secretion of metabolites to the extracellular space was enhanced by the presence of more microbes, thereby creating a larger concentration of extracellular polymeric substances containing proteins and polysaccharides [78].

Agricultural wastewater, including swine slurry, contains a high concentration of various pollutants, organic matter, nutrients, phenols, and heavy metals. The presence of heavy metals inhibited the growth of microorganisms in the swine slurry [79–81]. In CWMFCs, these undesired substances can be adsorbed by substrate layers modified with PAC. The anode potential reduced the PAC addition in the anodic chamber as the microbial growth was restrained. However, granular activated carbon behaved like an electron capacitor when used as a support material for exoelectrogenic bacteria. This study evaluated the effect of the distance between the anode and cathode on system performance by manipulating the depth of anode and cathode in up-flow CWMFCs. The electron transfer efficiency in the anode depends on factors such as the substrates and the probability of contact at the surface. Microbial growth is favoured at the cathode by the addition of PAC to form the biocathode and improve the performance [79]. The increase in PAC enhanced the resistance of the electrolyte while decreasing the anodic and cathodic resistances. The formation of biocatalysts enhanced the reduction reactions and decreased the resistance at the cathode. Similarly, the conductivity of the substrates at the anode was augmented due to the presence of PAC, which led to a reduction in the anodic resistance [82]. However, the electrode distance plays a pivotal role in the internal resistance of the system. A decrease in this distance reduced the IR of the device. The CE was found to be the highest with 2% of PAC.

Another CWMFC was designed using two stems of *Phragmites australis* and was tested for treatment of grey wastewater, where it removed 90% of the COD [83]. A comparative study for nitrate removal in wetlands indicated that the removal rate was 99% with CW reactors but 86% with CWMFC reactors. The nitrate and the anode compete to accept electrons in the CWMFC device; hence, most of the electrons were used to produce electricity instead of reducing the nitrate [84]. The anode respiring bacteria *Geobacter sulfurreducens* was found to be an

appropriate choice for enhancing the efficiency of this CWMFC system. The CWMFC was designed for treatment of greywater in batch cycle mode to eliminate phosphate, nitrate, and COD and enhance electricity production.

Another study compared the efficiency of double-chamber and single-chambered CWMFCs in paddy fields. [85] This study was conducted to treat wastewater generated from a fishery, where the double-chamber CWMFC was found to be more efficient. The tillering and seedling stage of the paddy field crops generated the largest amount of power due to excess exudates and high microbial activities. Thus, The vegetative stage was significant because it produced more current than the reproductive stage. Fewer rhizodeposits and formation of a thick biofilm towards the later stage reduced the current production. The efficiency of pollutant removal was enhanced because clogging (caused by the formation of the biofilm) was reduced due to the roots of the plants. Thus, the movement of protons was facilitated by the electrochemically active bacteria. The amino acids and carbohydrates present in the root exudates serve as a source of substrates for carbon production. Additionally, power production by the double-chamber CWMFC was also efficient. Another group reported powering an ultra-low-power receiver using a CWMFC, which could be applied in wireless technology as a future prospect. [86] The power from the CWMFC was sufficient to maintain the on-demand switch for the wake-up device. Additionally, a low-power wireless sensor was rebooted to the initial state after each interval. It is worth mentioning that the CWMFC placed outdoors provided more energy than that placed indoors. A double-chamber CWMFC was designed in which the inner cathode chamber was separated from the anode by a terracotta separator equipped with an air cathode assembly and paddy root matrix, which exhibited better efficiency [87]. This CWMFC, equipped with an internal cathode chamber and a separator-electrode assembly, was studied for the first time. This design reduced the cost of the system while enhancing the recycling process and water recovery. Bioelectricity can be generated by applying this technology in household terracotta pots and may aid in balancing the water-energy-food nexus.

In another study, a CWMFC was scaled up to treat 30 L of wastewater with four anodes immersed at different depths and one U-shaped cathode placed at the top, as shown in Figure 6, and removed 55% of the COD [88]. Aeration and circulation further enhanced the COD removal due to the increase in oxygen in the parallel mode of MFC connection. Additionally, the MFC connection mode is significant for eliminating COD. Under parallel connection conditions, COD removal was further boosted. In both combined and parallel connections,

cathodes with aeration and circulation showed less COD removal than those with only circulation. Aeration was hindered in cathodes with parallel and combined connections due to the consumption of dissolved oxygen (DO) at the MFC cathode instead of COD digestion. The thick biofilm layer at the water/ air interface and on the cathode prevented air diffusion. Thus, circulation and aeration enhanced the DO concentration, which influenced the nitrogen removal efficiency in the open circuit CWMFC, which was further enhanced in closed circuits.
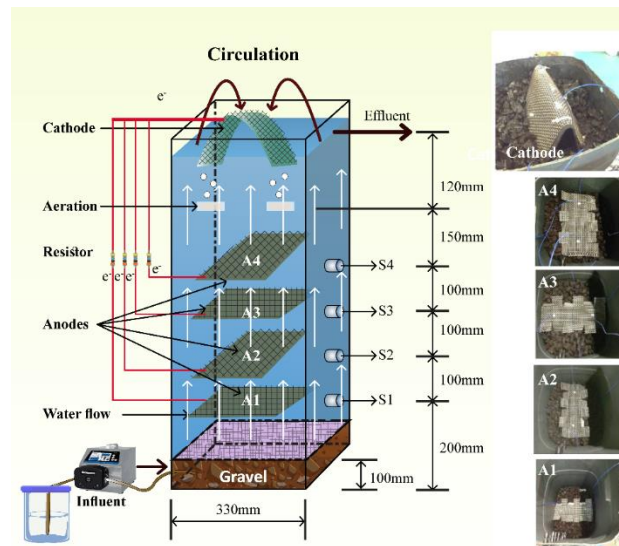


**Figure 6.** Schematic description of the pilot-scale CWMFC, actual photographs, and the anatomy of the electrode placement within the operation; figure adapted from a previous study [88].

The area of the cathode above the water remained dry, indicating that it was inactive. The raw system behaved simply as an up-flow CW. Circulation failed to introduce enough oxygen compared to aeration. The part of the cathode above the water was dampened after circulation, making it active by inducing oxygen diffusion to the required area. Thus, the synergistic effect of circulation and aeration was mandatory for improving the output of the system. A parallel connection with a multiple anode system was better than the combined anode system [89]. The IR of the MFC was dictated by the charge transfer resistance between the electrodes and the surface resistance of the electrodes.

Three different types of wastewaters were studied using a CWMFC to generate bioelectricity, which proved that an efficient current could be generated in the presence of nutrients as influents [90]. However, nitrate-free wastewater showed the best output, although the CE was low for all of the systems. Heterotrophic microorganisms and the EAB are abundantly present in the CWMFC, which uses organic matter in synthetic wastewater for electricity production.

Thus, alteration of the microbial community at the anode due to different wastewater does not affect its performance. The active carbon granules have excellent adsorption capability, which shows good COD removal efficiency, especially nitrate with a carbon anode. Ammonium was removed from the air cathode. The microbial community at the anode consisted of *Desulfobulbus, Geothrix, Geobacter,* and *Desulfovibrio*.

In another study, an integrated vertical flow CW (IV-CW) was assembled with a MFC for treatment of swine wastewater, and the energy for pumping the influent was decreased due to a larger difference in the gradient of the redox potential [91]. The COD removal efficiency (COD$_{EF}$)was higher in the closed circuit system than the open circuit system because the anode acts as the electrode acceptor and aids in anaerobic treatment [92]. The IV-CWMFC exhibited an aerobic-anaerobic-aerobic process in which the microbes at the roots of *Canna indica* degraded organic matter and nitrogen. The electrogenic bacteria used hydrolytic products such as acetic acid etc., to remove pollutants [93,94]. The anode improved the growth of the biomembrane, thus reducing the COD. The internal resistance was low due to good conducting electrodes and a continuous flow of water [95]. The low CE value was attributed to the dynamic transfer limit due to the resistance in charge transfer based on the sluggish rate of activation at the electrodes. The microbes were identified as *Desulfuromonas* and *Geobacter.*

Degeneration of nitrobenzene-containing wastewater was carried out using a CWMFC with water hyacinth (*Eichhornia crassipes*) as the plant species and showed improved bioelectricity production [96]. The roots of the water hyacinth plant provided the required oxygen to the cathode and increased its efficiency [97]. Because the internal resistance of CWMFC is affected by the spacing of the electrodes, the optimum distance was maintained at 13 cm. The anaerobic bacteria converted the nitrobenzene to aniline, which was removed efficiently by the system. Additionally, nitrobenzene was also absorbed and deposited in the rhizosphere of the plants.

A membraneless CWMFC was fabricated with graphite and gravel as the anode constituents to treat domestic wastewater [98]. The response time is paramount for biosensing tools used in real-time monitoring [99]. The system with graphite and gravel anodes exhibited better values of $R^2$ because the prolonged time (20 h) of the organic matter within the system led to more degradation of the organic matter. The contact time was significant for organic matter with low concentration. Additionally, the organic matter used for electricity generation came from both the influent and the organic matter prevalent in the anode chamber. COD detection was better

with graphite, and the pilot plant examination demonstrated that the cell potential was enhanced with the augmentation of the organic matter concentration.

The naturally occurring redox gradient between the organic sediments and surface water was exploited to design a green MFC known as the sediment or benthic or marine-rooted plant MFC (MPMFC) [100]. The introduction of plants into the MPMFC led to the development of the CWMFC. The basic principle of the CWMFC is to obtain energy by placing the anode in de-oxygenated sediment near the roots of the plants and placing the cathode in the oxygenated water above, as shown in Figure 7. The plants provide the carbon source to the anode-adhered EAB, and thus, regulating the water flow in the wetlands results in a constant supply of carbon and absorption of contaminants by the plants for their growth [101].
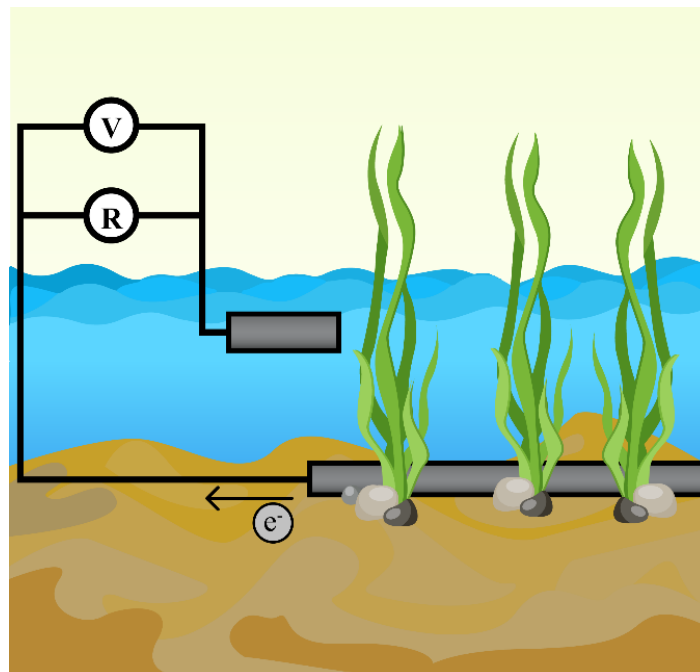


**Figure 7.** A schematic representation of constructed wetland microbial fuel cells (SMFC) and application of the SMFC system in a (constructed) wetland. The anode matrix is positioned in the root zone and the cathode in the overlying water layer; figure adapted from a previous [101].

Grass-like plants that grow with their roots submerged in water provide the necessary anerobic conditions for the anode-adhered EABs in NPMFCs. It was found previously that the voltage was higher in the NPMFC to which compost was added. The addition of compost boosted the growth of plants, and the soil microflora was also enhanced, thereby augmenting the NPMFC function [102]. NPMFC start-up operation increased the soil temperature by 10°C, which resulted in a decrease in the kinetics of soil heterotrophic bacteria by up to 30°C and stimulated photosynthesis [103]. NPMFC also been shown for 0.3 nmol d$^{-1}$ per m$^3$ hydrogen production [104].

Four different wetland plants, namely, *Cyperus alternifolius L., Acorus calamus, Canna indica,* and *Arundo donax*, were examined for use in a CWMFC [105]. *Arundo donax* was found to be suitable due to low IR, good adaptability, and long-developed roots that could clean sewage water efficiently. The $COD_{EF}$ of different CWMFC are shown in Table 3.

**Table 3.** Efficiency of COD removal ($COD_{EF}$) by various CWMFC.

| Plant species | $COD_{EF}$ (%) | $P_A$ (mW m$^{-2}$) | Ref. |
|---|---|---|---|
| *Phragmites australis* | 76.5 | 9.4 | [106] |
| *Phragmites australis* | 64 | 28 | [107] |
| *Phragmites australis* | 87 | 33 | [83] |
| *Ipomoea aquatic* | 94.8 | 30.2 | [108] |
| *Canna indica* | 75 | 15.7 | [109] |
| *Iris pseudacorus* | 99 | 9.6 | [110] |
| *Typha latifolia* | 91.2 | 93 | [111] |

**3.1 Factors affecting CWMFC in wastewater treatment**

The factors affecting wastewater treatment using an up-flow CWMFC system were studied by designing an orthogonal experiment [112]. Thus, the optimal operating conditions were identified for standardizing the elimination of nutrients and organic matter in CWMFCs. The granular graphite volume ratio was altered in the substrates, and parameters such as external resistance, concentration of DO in the cathode compartments, and HRT were considered. The treatment efficiency of pollutants was augmented by returning the effluent to the systems. The anaerobic environment of the anodic cell was influenced by the refluxed effluent, which affected the output of the system and prompted a study on the influence of the effluent's reflux ratio. The HRT, reflux of the effluent, and concentration of DO play vital roles in the removal of $COD_{Cr}$, nitrogen-$NH_3$, and TN, respectively. TN removal was exclusively affected by the volume ratio of the granular graphite and external resistance. The contact time between the microbes and the substrates was enhanced by increasing the HRT, whereby the reaction time for degradation of the pollutants through adsorption could also be improved [113]. The removal efficacy of pollutants increased up to a threshold limit on enhancing the HRT. Beyond the threshold limit, the efficiency is reduced as the anaerobic condition is exacerbated in the CW. The reversed

effluent enhanced the HRT by diluting the wastewater influent and improved the removal of pollutants. The introduction of DO at the bottom of the CWMFC increased the aerobic degeneration of the organic compounds. The nitrogenous compounds were removed by denitrification of the anodic compartment. Optimal performance was reported with a 50% reflux ratio of effluents. The presence of the MFC, along with the CW, increased the nitrobacteria and beta-Proteobacteria. Additionally, the presence of denitrifying bacteria was increased in the CWMFC with a closed circuit. The output voltage obtained from the CWMFC increased with enhancement of the external resistance while the current was reduced. Additionally, a rapid rate of consumption of the organic compounds by the electrogens increased the current [114]. However, the low current provided fewer electrons for the denitrification process at the cathode. Thus, an increase in the external resistance reduced the removal of nitrogen and organic compounds in the CWMFC. However, the removal of P was not affected by the MFC but was influenced by the physicochemical process of the substrates [115]. The electron acceptor in the MFC is increased by enhancing the concentration of the DO in the cathode zone, which produces high electricity through aerobic degradation of the organic compounds [116]. Nevertheless, a high DO concentration negatively affected the aerobic environment within the anodic cell, which negatively impacted power generation [117]. The concentration of DO should be appropriate for pollutant elimination and electricity generation. The porous nature of the graphite increased the concentration gradient of DO in the cathode zone, which influenced the anaerobic and anoxic microenvironment within the aerobic area of the cathode. Thus, an increase in the amount of granular graphite enhanced the removal of nitrogen in the CWMFC.

### 3.2. Flow patterns in CWMFCs

Wastewater flows into the wetlands by two different hydrological patterns, namely, subsurface flow and surface flow, and subsurface flow is favored for the CWMFC [113]. The organic materials move into the anode through subsurface flow, and the effluent finally moves into the cathode, thereby separating both electrodes. The combination of the flow in the anode and the down-flow in the cathode in the CWMFC can be tuned to enhance the power output in the devices [79]. The major disadvantage of this system is that elimination of organic compounds was decreased compared to devices with up-flow patterns. Additionally, the growth of heterotrophic bacteria on the cathode was increased, which used up the oxygen in the cathodic chamber. Thus, the amount of oxygen for autotrophic bacteria is limited for catalysis of the reaction to reduce oxygen. However, horizontal flow is preferred for large-scale devices [118].

A study was conducted to optimize the relationship between the electrode distance and the flow regimes; in the CWMFC in this study, the cathode was buried, and swine wastewater was treated [107]. Graphite granules were used as electrodes. Issues such as the requirement for an anoxic condition at the anode and aerobic conditions at the cathode and the separation between the electrodes were overcome by introducing up-flow and down-flow simultaneously in the CWMFC. Moreover, the power density was improved as the IR was diminished due to the up-flow and down-flow movement.

## 3.3. Modified constructed wetland microbial fuel cells

### 3.3.1. Biofilm electrode reactor coupled to constructed wetland microbial fuel cells

A biofilm electrode reactor (BER) was operated with the aid of a stacked MFCCW for reduction of the antibiotic-reducing genes and antibiotics (SMX), as shown in Figure 8 [119].
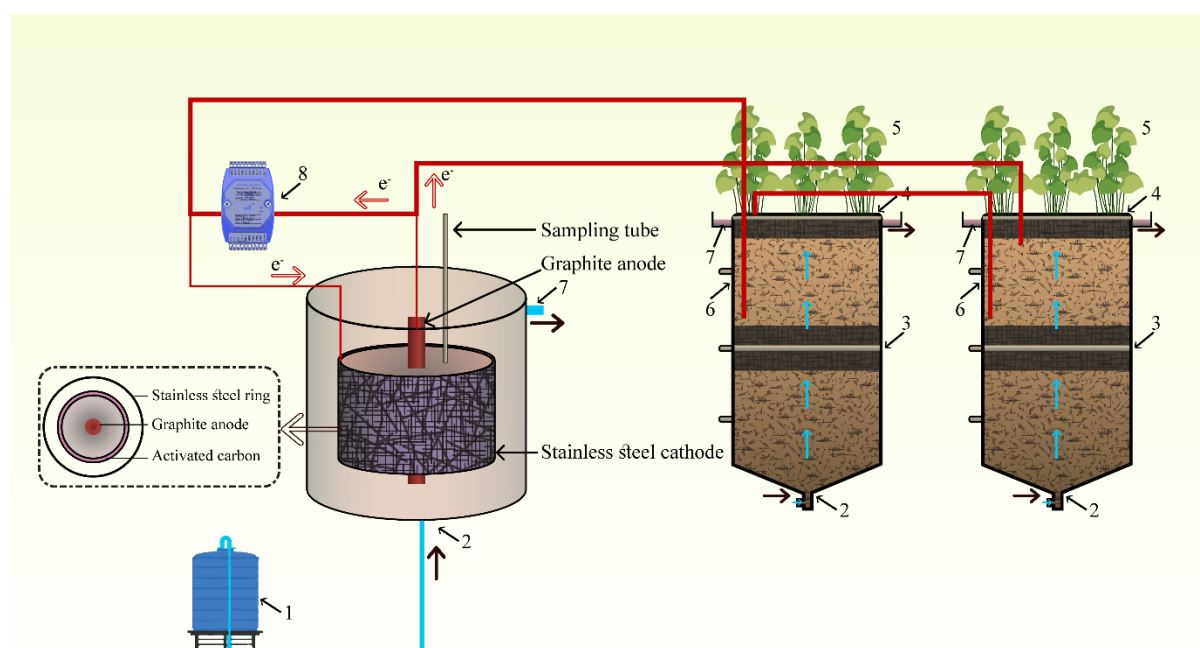


**Figure 8.** Schematics of continuous flow biofilm electrode reactor microbial fuel cell–constructed wetland (BER-MFCCW) and its associated components; figure adapted from a previous study [119].

The concentration of the SMX was decreased by using BER as a pre-processing unit. The effluent could enter the MFC-CW system, where the SMX was degraded completely, leading to diminishment of the antibiotic reducing genes. The power required by the BER was supplied by two MFC-CW units connected in series. Additionally, bioelectricity generation was not

25

decreased even in the presence of a high concentration of SMX. The SMX was degraded in the BER system by electrons moving from the anode through wires, which augmented the removal of glucose and SMX due to the improved activity of the microorganisms [120]. The higher voltage in the stacked unit improved the efficiency of the removal of SMX. The BER system maintained the stability of the complete system. The enhanced removal rate was attributed to sorption of the substrate layer, microbial degradation, and hydrolysis [121]. The anode removed the maximum amount of SMX (42–55%), with 20% removal by the bottom layer, whereas the cathode and the middle layer removed approximately 1%. Thus, the ARGs and bacteria were effectively inhibited in the MFCCW unit. The COD was due to the biorefractory compound (SMX) and the co-substrate (glucose). The effluent in the BER remained a high amount of glucose when operated at low HRT, whereas more glucose was consumed when the HRT was longer. There was no voltage reversal issue with the system.

### 3.3.2. Microbial electrosynthesis coupled to constructed wetland microbial fuel cells

The density and community of the microbes, along with the purification of sewage water, were studied in another CWME system, which consisted of graphite electrodes and *Eichhornia crassipes* (water hyacinth) [122]. The application of high voltages facilitated removal of the nitrogen in ammonium ions in the anode under anaerobic conditions [123]. The reduced diffusion of oxygen transforms the $NH_4^+$-N to $NO_3$-N that is used in the reduction of autotrophic N on the cathode [124]. Accordingly, sulphates and phosphates and COD were also removed. Bioelectricity was generated by oxidizing the organic matter available in the sewage water. The microbes present in the system were predominantly *Bacteroidetes, Proteobacteria, Actinobacteria,* and *Firmicutes/Bacillota.*

### 3.3.3. Capacitors

Another group enhanced the efficacy of the CWMFC by adding external capacitors, which were also applied to scale a multi-electrode CWMFC [125]. The frequency of charging and discharging (D) plays a pivotal role in the efficiency of the system because an enhanced TOV is obtained with a lower D value. Additionally, for a system with high IR, as in the case of the CWMFC, the loss in voltage can be eliminated using the CDC operation mode. Thus, the electrons generated during oxidation were stored in the capacitors. The charge release at a high rate generates a potential gradient at the biofilm on the anode, which increases the charge transport within the biofilm matrix [126]. COD was removed at a faster rate in DC/CDC mode.

## 4 Marine-rooted plant microbial fuel cells

Marine-rooted plant microbial fuel cells (MPMFCs) are used in a natural system like CW and work on the natural oxygen gradient principle, which separates the anode from the cathode instead of a membrane [127]. The electrode of the cathode is placed in water. Simultaneously, the anode is immersed in the sediment and placed in the vicinity of the rhizosphere of plants so that the organic compounds eliminated by the roots can be utilized [128,129]. The power output of the MPMFC is low based on its high internal resistance and the inadequate supply of electron acceptors and donors. Conversely, the maintenance of this system is minimal, which is an asset for its use in deep waters. *Phragmites australis* and *Ipomoea aquatica* are two plants that are mainly used in MPMFC. The efficacy of the MPMFC is enhanced due to the increased level of DO, which is attributed to the plant roots [79]. The microbes in the cathode are augmented due to the presence of plants, with a slight increase in the population of *Geobacter sulfurreducens* at the anode. Figure 9 gives a schematic representation of the experimental setup used in the study. In this study, four different types of architecture were tested to check the optimum arrangement, such that the internal resistance can be reduced by reducing the electrode space.

The two main species of bacteria present in the soil are *Geobacter* spp. and *Shewanella* spp., which produce electricity and can metabolize minerals such as lead and iron in the soil. In one study, the soil from barren land was added in three different MFC units and stacked in parallel and series using titanium wires. Although power was generated, the output was low in the MFC set-up, and there is ample room to improve the system architecture for enhanced performance [130]. Figure 9 shows a schematic of the marine-rooted plant MFCs.
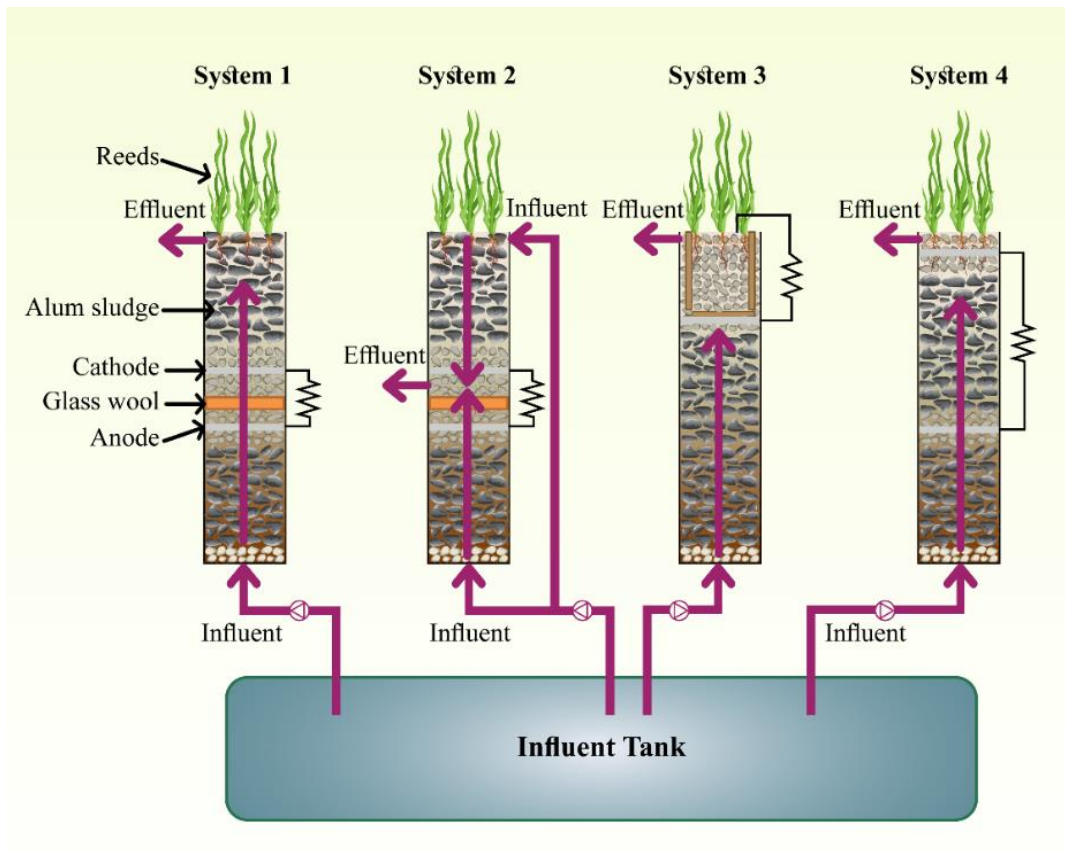
**Figure 9.** Schematic representation of the experimental setup for the marine-rooted plant MFC with four variable configurations to understand the overall performance of the system; figure adapted from a previous study [79].

## 5 Algae-based microbial fuel cells

Algal-based MFCs are based on cathode inhabiting algae (ACCC) and anode inhabiting algae (AAMFCs), with the latter being further categorized based on the solar energies being captured and the transfer mechanism of organic molecules and electrons.

### 5.1 Anode algal microbial fuel cells

MFCs with algae in the anode chamber containing an EAB can produce substrate molecules as by-products or from the algae themselves after lysing, this can simplify the operation of the system to allow development to focus on light management. In addition, consumption of $CO_2$ in the anode chamber can help deacidify the EAB growth environment, however the production of $O_2$ in the anode chamber can harm EABs, which is likely the main reason these variants of algal MFC are less represented in the literature compared to ACCC (algae in the cathode). However, there are recent examples of AAMFCs, including those in which algae are cultured directly on the anode and electrons are extracted directly from the photosynthesis metabolic

process or related photochemical processes. AAMFCs also show a potential for use as sensors due to a noted sensitivity toward contaminants present in water, such as pharmaceuticals and herbicides [131].

A humidity-preventive membrane electrode assembly (MEA) was used in the design of a vertically stacked triple-chamber AAMFC in which the PEM was fabricated using a hot press [132] to sandwich stainless steel anodes between two cathodes, as shown in Figure 10. The electrodes were fabricated as a mesh type with a large surface area, and the transparency was optimized by altering the pitch and diameter of the mesh. *Microcystis aeruginosa* was used as the green algae species, and thus the power density was increased compared to a single cathode chamber.
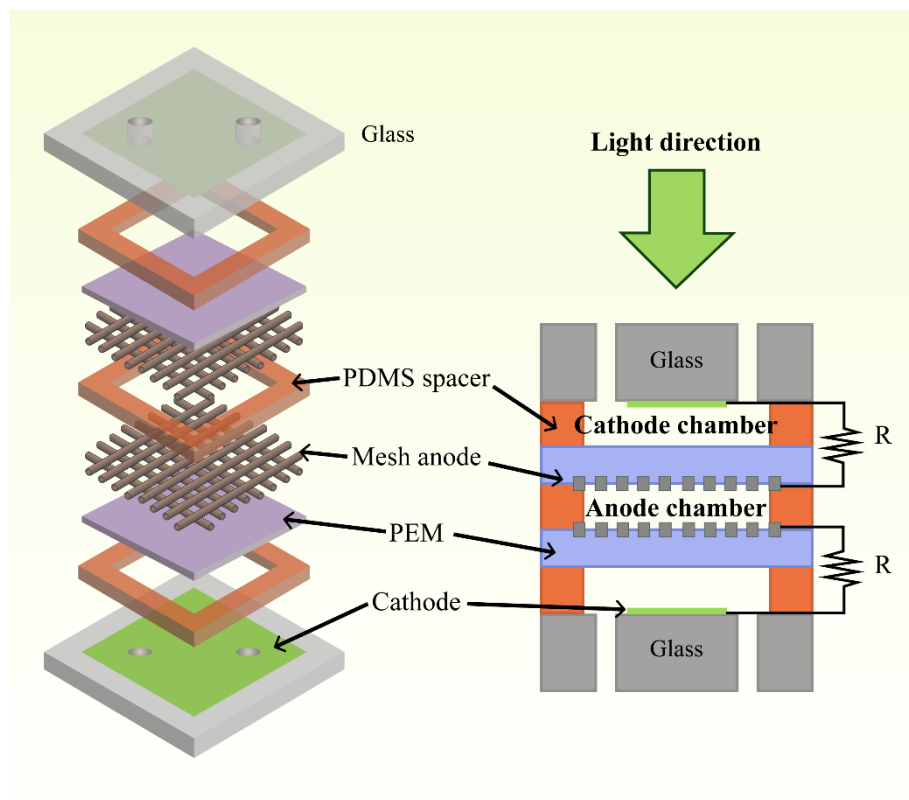


**Figure 10.** Graphical representation of a dual-cathode chamber (stacked) algal microbial fuel cell with internal components; figure adapted from a previous study [132].

The use of Pt catalysts at the cathode is essential for the effective reaction process and production of current density [133]. A study was conducted in the absence of the Pt catalyst using carbon-based air cathodes operating in batch mode, such that the surface area of the cathode

was immersed in the solution. Carbon cathodes were designed by attaching different carbon materials to the PEM (Nafion 115) using a hot pressing process, and ZACC FM10 was found to be effective [134]. The anode was fabricated from ceramic with a similar cathode surface area. The power density of the device was a function of the anode surface area. Electrochemical analysis of the internal electrode surface area is carried out by measuring the capacitance of the double layer of a particular sample composed of similar material with a known surface area [135]. The active surface area of the cathode dictates the difference in the power output of an AAMFC. The surface area of the carbon paper was very low, whereas carbon felt could not endure the hot-pressing procedure because the interconnecting carbon fibres were destroyed. However, ZACC FM10 exhibited durability under high pressure. The cathode was examined in a flow AAMFC in the absence of redox mediators with a ceramic anode coated with $TiO_2$ in the presence of *C. emersonii,* and *Synechocystis* spp. PCC 6803 as the microbial culture generated a considerable amount of power output.

An AAMFC was developed in which the efficiency of different cultures of algae-like *Nannochloropsis, Spirulina*, and *Chlorella* was studied, among which *Nannochloropsis* was found to be effective because it proliferated over a long duration along with an electricity generation of 35 mW [136]. However, the photometric absorption rate for the other two species was lower, exhibiting a diffusion limit and diminishing their power output efficiency. The PEM was fabricated using a mixture of electrolytic polymers.

A portable paper-based MFC was designed using purple photosynthetic bacteria to form a dry surface biofilm [137]. A very thick biofilm did not yield effective performance because oxygen diffusion was hindered. The bacterial load varied in various electrodes, and the size of the bacteria cells was 2–3 µm. The bacteria population was greater on the carbon nanotube-coated electrodes compared to that on the carbon-coated electrodes. Additionally, the ozone-treated electrodes exhibited better performance due to enhanced hydrophilicity, thus enhancing the ability to absorb water. Thus, ozone-treated CNT-coated carbon electrodes exhibited better performance in the MFC [137].

In another study, the cathode in the AAMFC was inoculated with the eukaryotic microalgae *Scenedesmus obliquus* and treated Atrazine by monitoring alteration in the DO levels in the catholyte [138]. The production of hydroxide enhanced the pH of the catholyte, which finally enhanced the amount of DO and hindered the growth of heterotrophic bacteria and produced a

lower current. Other factors influencing the low output of the system were the crossover of oxygen to the anode, the absence of catalysts, the low conductivity of the electrolytes, and an excess amount of DO. The response time to atrazine was weak due to the dense biofilm on the surface of the ITO, which hindered the identification of the DO. A summary of results from some prominent anode algal MFCs studies for power production, the duration of active microbes and other properties are given in Table 4.

1    **Table 4.** Summary of power production in anode algal microbial fuel cells (AAMFCs).

| AAMFCs Type | Anode | Cathode | Duration (days) | $P_A$ (mW m$^{-2}$)* | CE (%) | COD$_{EF}$ (%) | Ref. |
|---|---|---|---|---|---|---|---|
| Dual-chamber | *Chlorella. regularis* | PBS (50 mM, pH = 7.2) | 33 | 1070 | 61.5 | 65.2 | [139] |
| Dual-chamber | *Spirulina platensis* | Tapioca wastewater | 192 | 14.47 | NA | 67 | [140] |
| Dual-chamber | *Microcystis aeruginosa* | Potassium ferricyanide (50 mM) | 600 | 83 | 7.6 | 67.5 | [141] |
| Dual-chamber | *Chlorella pyrenoidosa* | Potassium ferricyanide | 5 | 6030 | NA | NA | [142] |
| Sigle chamber | *Synechocystis spp.* | BG11 | 19 | 10 | NA | NA | [143] |
| Sigle chamber | *Chlorella emersonii* | Air cathode | 6 | 7.4 | NA | NA | [134] |
| Sigle chamber | Photosynthetic pond culture/BG 11 | Air cathode | 8 | 3,4 | NA | NA | [144] |
| Sigle chamber | Natural hot spring community | Air cathode | 8 | 9 | NA | NA | [145] |

2

## 5.2. Cathode considerations in anode algal MFCs

To a large degree, the anode material dictates the power density, however, in the absence of Pt at the cathode, which is an efficient surface of oxygen reduction reaction, the reaction on the surface of the cathode may become rate limiting [133]. Carbon-based cathodes with a large surface area of fibrous carbon can be used in AAMFCs, where the cathode was hot pressed and attached to the PEM, but this can reduced the electroactive surface area [134]. To measure the total electroactive surface area of the electrode, a double-layer capacitance measurement can be made and comparied with the same from a sample with a known surface area [135]. By this method, ZACC FM10 + Nafion 115 was revealed as the most effective air cathode, and was found to delivered highest voltages, whereas cathodes with low surface area carbon paper generated the lowest power density.

## 5.3. Flow cells in the absence of an artificial redox mediator

In some biophotovoltaic cells, power can be generated by extracting electrons directly from photosynthetic metabolic processes and related photochemical processes, but this often requires a mediator, since extracellular electron transport is usually not supported. This can present certain disadvantages, since mediators can be toxic and expensive. Thus a flow-cell AAMFC was examined in the absence of redox mediators by using porous $TiO_2$ ceramic anodes and air cathodes in the presence of *Synechocystis* sp. PCC 6803 and *C. emersonii* as cultures [134]. The anode was covered with a green biofilm, which produced higher voltages during the day than during the dark night period, and the voltage obtained from *C. emersonii* was ten times lower.
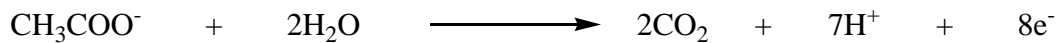
## 5.4. Algal carbon capture cells

Algal photosynthesis is developed with an ACCC in which oxygen is generated *in situ* through the photosynthesis of algae within the cathode compartment [146,147]. An ACCC is algal-MFC variant that facilitates terminal electron reduction in the MFC using $O_2$ produced by algae in the cathode chamber. This can increases power production while simultaneously removing $CO_2$, which is produced from degradation of the substrate in the anode chamber [148,149]. Thus, AAMFCs have been used for current production and wastewater treatment, which requires an uninterrupted supply of $CO_2$ to the cathode chamber [131]. In the absence of aeration, $CO_2$ emission is effectively curtailed with a promising voltage output in ACCCs [150,151]. After the MFC is operated for a certain period, a film of electrochemically active bacteria is formed on
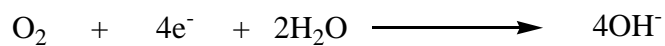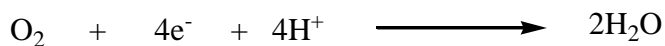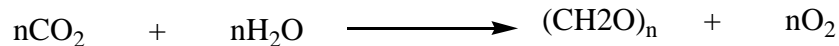
the anode, and a biofilm of algae is formed on the cathode. The parameters affecting the cathode chamber in ACCCs are mainly pH and DO, and $CO_2$ crossover takes place through the PEM to the cathode chamber from the anode [152].

The reactions taking place in the photocathode chamber includes primarily the reduction of oxygen produced during photosynthesis, reduction of $CO_2$, and transfer of electrons through the self-produced mediators. Among the three reactions, the most significant is the reduction of oxygen to form a hydroxyl anion [153] due to photosynthesis in the ACCC, where the rate of production of oxygen depends on the $CO_2$ absorption rate by the algae. The reaction at the anode and the cathode is shown in Scheme 1.

At anode

$$CH_3COO^- + 2H_2O \longrightarrow 2CO_2 + 7H^+ + 8e^-$$

At cathode

$$nCO_2 + nH_2O \longrightarrow (CH2O)_n + nO_2$$

$$O_2 + 4e^- + 4H^+ \longrightarrow 2H_2O$$

$$O_2 + 4e^- + 2H_2O \longrightarrow 4OH^-$$

**Scheme 1:** Reaction occurring at the electrodes in an ACCC.

In general, the experimental oxygen reduction reaction potential can be higher than the theoretical oxygen reduction reaction potential due to the formation of alkali at the cathode. This can be improved by lowering the pH in the catholyte chamber, which is achieved by enabling the diffusion of $CO_2$ and protons from the anode chamber [154]. The working principle is shown in Figure 11.
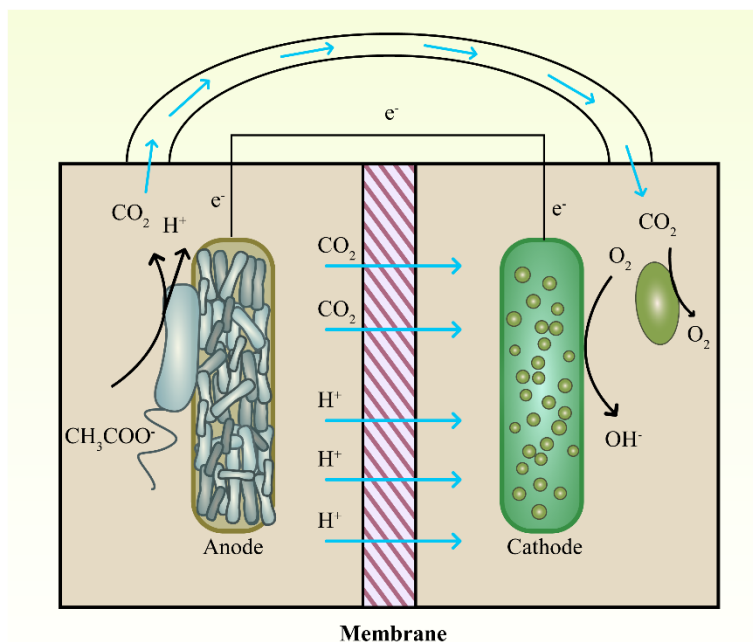
**Figure 11.** Working principle of the algal carbon capture cell (ACCC); $CO_2$ transportation and EAB anode and algal-based cathode reactions are involved. Figure adapted from a previous study [155].

A PhMFC that behaved like an ACCC was designed using polybenzimidazole (PBI) as the membrane and a biocathode with a pure culture of *Scenedesmus acutus* microalgae and domestic wastewater as the anolyte. The algae in the biocathode produced oxygen through photosynthesis. The microalgae used the $CO_2$ generated from the degradation of the wastewater at the anode for photosynthesis, thereby producing oxygen. This study examined the performance of two ACCCs in which the gas diffusion electrode at the cathode was made of Pt and the other was free of Pt [156]. The PBI composites also inhibited the adhesion of microbes, which helped in preventing membrane biofouling; also, the membrane was resistant to structural and mechanical degradation. The PBI composites also inhibited the adhesion of microbes, and thus, the problem of membrane biofouling was improved. The biofilm deposited on the anode was stable in both cases. The electrocatalyst (Pt) presence accelerated the oxidation-reduction reaction and produced excess power and better COD removal. The loss of performance was more noticeable in the ACCC with the Pt catalyst because agglomerates were deposited during the electrochemical process, thus blocking the electroactive sites on the surface. The oxidative stress condition of the microalgae within the device led to the accumulation of bioactive substrates such as lutein and fatty acids, which aided in their survival over a long duration of time [157].

Significant factors dictate the output of an ACCC, whereby both the photobioreactor and the MFC mutually gain an advantage. Thus, a statistical evaluation was conducted by adopting the Box-Behnken design to assess parameters such as the concentration of the lipid-extracted algae (LEA) of the various microalgae cultures present in the anodes and the concentration of nitrates in the catholyte [158]. Although there is no interactive effect among the parameters (LEA, photoperiod, and nitrate) on the power density, each parameter exhibits significant individual effects. The growth of the algae depends on the duration of light and the concentration of nitrate. The concentration of the DO in the cathodic chamber is again influenced by the growth of the algae, which affects the capacity of power production [159]. There is a saturation concentration for the DO in the catholyte [160]. Thus, the effect of the parameters on light generation becomes insignificant after the catholyte reaches the saturation concentration. The duration of light influences the productivity of the algae because it dictates nutrient uptake.

A miniature single-chamber ACCC was designed with an air cathode to identify toxic compounds in water [161]. The system was supplied with the flow, which enhanced the current, proving that adequate nutrients were mandatory for the electrogenesis process. Additionally, the current output was greater during the day, indicating that the electron source is the photolysis of water. Again, the heterotrophic bacteria present in the biofilm oxidize the organic compounds eliminated by the microalgae to generate electrons. These two effects of heterotrophic microorganisms and photosynthesis are synergistic in the process.

The reduction in current was attributed to the accretion of DO in the anodic chamber with a gradual enhancement of the pH value to 9 [162]. The system exhibited high internal resistance and was used to detect formaldehyde. The accumulation of bacteria was higher in the portion exposed to formaldehyde because the microalgae present in the biofilm became detached in the presence of formaldehyde.

A summary of results from some representative algal carbon capture cells is given in Table 5.

**Table 5.** Summary of power production in algal carbon capture cells (ACCCs).

| ACCC Type | Anode | Cathode | $P_A$ (mW m$^{-2}$)* | [DO] (mg L$^{-1}$) | CE (%) | COD$_{EF}$ (%) | Ref |
|---|---|---|---|---|---|---|---|
| Dual-chamber | Activated sludge | *Chlorella vulgaris* | 2.5* | NA | 9.4 | 84.4 | [163] |
| Dual-chamber | Pre-acclimated (from domestic wastewater) | *Chlorella vulgaris* | 5.6* | 7.6 | NA | NA | [148] |
| Dual-chamber | Wastewater | *Scenedesmus obliquus* | 153 | 15.7 | NA | NA | [164] |
| Sediment | Sediment | *Chlorella vulgaris* | 38 | 5.8 | NA | NA | [165] |
| Tubular | Anaerobic sludge from a wastewater treatment plant | *Chlorella* | 6.4 | NA | NA | NA | [166] |
| Dual-chamber | Cow manure | *Chlorella vulgaris* | 2.7* | NA | 0.0782 kW h m$^{-3}$ | 0.0136 kW h kg$^{-1}$ | [167] |
| Dual-chamber | Bacterial consortium with the previously enriched anode | *Chlorella vulgaris* | 62.7 | NA | NA | NA | [150] |
| Dual-chamber | Activated sludge | *Chlorella vulgaris* | 126* | 9.5 | 70 | 5.47 | [168] |
| Dual-chamber lagooning | Activated sludge | Mixed Microalgae | 12.6* | 8 | NA | NA | [169] |
| Single-chamber | Textile wastewater | *Chlorella vulgaris* | 123.2* | NA | 19 | 98 | [170] |

| A concentric cylinder | Anaerobic sludge | *Chlorella vulgaris* | 390 | 3800 | NA | NA | [171] |
|---|---|---|---|---|---|---|---|
| Dual-chamber | Swine wastewater | *Chlorella vulgaris* | 3720* | NA | NA | NA | [172] |

* Volumetric power density (mW m$^{-3}$)


## 7. Advantages and challenges of phototropic MFCs

The major challenge associated with PhMFCs is maintaining the electrode function over a long duration and maintaining the plants and algae. Thus, an analysis of the microbes and their area of existence is mandatory for enhancing the electrochemical performance of PhMFCs. The presence and location of EAB is a major consideration, in this respect. For example, a metagenomic and molecular phylogenetic survey of some plant-based PhMFCs together and their respective rhizospheres, indicated that the EAB present in the anodes of the glucose-fed MFC and rhizosphere PhMFC is similar in many aspects and produces electricity by a similar mechanism [69]. Electricity is generated by the EAB from rice plants and fermentative bacteria in the rhizosphere PhMFC and glucose-fed MFC through syntrophic interaction. Electrons are donated by acetates from the roots of the rice to the EAB in the rhizosphere PhMFC. This aids in the prevalence of the *Geobacter* EAB. In another the ubiquity of EAB was again demonstrated, this time showing that the EAB covered both the surface of the roots of *Glyceria maxima*, and the granular graphite electrode [63]. Because anaerobic cellulolytic bacteria were also present at these sites, cellulosic hydrolysis produced the current in the cell. The graphite granules accepted electrons in this system, and methanogens that use acetate were not as active as electron donors.

In one study, *Eichornia*, the abundant microbe, showed good performance in a floating macrophyte-based ecosystem [65]. The O$_2$ required for bacteria is acquired from nitrate or DO. Denitrification occurs when bacteria consume DO, and nitrate becomes the sole O$_2$ source for bacteria. The concentration of DO was dictated by *Eichornia* and the amount of sunlight. The level of DO increased throughout the day and reached a maximum in the evening due to the photosynthesis by *Eichornia.* This variation of DO from morning to evening is an asset because it initiates the growth of nitrogen-removing bacteria and substrate-degrading bacteria.

PhMFC also shows promise as a tool to remediate heavy metals present in the wastewaters. Cr (VI) was eliminated *in situ* using *Lolium perenne* as the plant in PhMFC, where the cost of operation was substantially decreased using a combined technique of bioelectrochemical phytoremediation [66]. Cr(VI) uptake by plants was considerably enhanced by this method. The plants in which Cr was deposited can be collected and incinerated after a specific duration, which is a green method of removing Cr from the system. However, the recovery of Cr from the electrodes requires further improvement. Additionally, a very concentrated level of toxic Cr (VI) has adverse effects on plants and microbes. Hence, the level of Cr(VI) tolerance for microbes and plants should be accurately analyzed to obtain the optimum efficacy. A study demonstrated the remediation of Cu-contaminated sediment using *Ipomoea aquatica* in PhMFC. The remediation was shown in the form of $Cu^{2+}$ to Cu nanoparticles on cathode site while generating electricity through the existence of root exudates [173]. A PhMFC based on *Ipomoea aquatica Forsk* was used to treat azo dye. The study demonstrated decolorization efficiency and COD removal of up to 99.64% and 92.06%, respectively [174]. Mishra et al, 2022 reported the use of *Dunaliella salina* to treat saline water for the first time [175].

Another study [35] reported evaluating concurrent biomass and electricity generation using *S. anglica* and *A. anomala* in two separate PhMFCs. Both systems generated an equal amount of electricity, but the maximum power production differed. This phenomenon was due to the influence of the membrane potential of each microbe on the density of current. A smaller membrane potential boosts the movement of ions across the membranes. A PhMFC with plants from salty water (*S. anglica*) is better because these plants have abundant ions obtained from the salts, thereby lowering the membrane potential compared to a PhMFC with plants from fresh water (*A. anomala*). Rhizodeposits from paddy plants were used in the construction of a PhMFC [67], establishing the fact that electricity can be produced from wetland crops. The substrate is oxidized to methane during current generation, and this technology offers great potential for power production in remote areas. This system is devoid of any costly techniques and unwanted reactions such as metal methylation.

Several studies showed that methane emission can be mitigated by PhMFCs by introducing a bioelectrochemical anode in the rhizosphere for current production via microbial metabolism [70]. However, the presence of excess organic constituents can boost methane production during the crop-growing season. This problem can be solved by constructing a bioelectrochemical system on a pilot scale. Moreover, it was found that hydrogen was a significant precursor for

methane generation in the anode, which can be addressed by increasing the competition for hydrogen at the acetoclastic methanogenesis level. A lifecycle analysis of a CWMFC revealed that an anode consisting of gravel negatively impacted the environment compared to a graphite anode or a conventionally constructed wetland system [176]. Thus, a graphite anode is preferred for constructed wetland MFC systems and decreases the footprint by 20%. Nevertheless, this system is more expensive than the conventional CW system.

The abundance of oxygen that is produced by algal photosynthesis at the cathode of an ACCC can be helpful not only for root growth, but the reactive nature of molecular oxygen can also be exploited for soil decontamination. *Scenedesmus obliquus* (a photoautotrophic algae) generated oxygen for electricity production by adhering to the cathode surface of an MFC [164]. In contrast, *Chlorella vulgaris* (another algae) was used to produce oxygen at the cathode in PhMFC [165]. The reduction rate of oxygen and the DO concentration were enhanced at the cathodes by photosynthetic algae. Another photosynthetic MFC was fabricated with stainless steel as a cathode, and the microbial colony was analyzed, revealing the presence of *Chlorella* in abundance. After multiple operations, the algae were retained on the electrode and actively initiated the oxygen reduction reaction when illuminated [166]. Lipids from cathode-harvested algae were extracted and used as substrate in an MFC, which exhibited more efficacy than fruit-waste-fed MFCs. A biocathode composed of microalgae showed substantial improvement compared to one containing platinum. The biocathode can be exposed to air and showed good potential for treating dye wastewater from textile industries [170].

## 8    Future perspectives and conclusion

This review summarizes the use of different phototrophic MFCs (PhMFCs), including plant- and algae-based systems, to produce bioelectricity and detect toxic substances in various wastewater sources. Compared to traditional MFCs, which produce $CO_2$ during substrate oxidation and consume $O_2$ at the cathode to complete the redox cycle, PhMFCs are a route to achieving true carbon neutrality. To maximize their benefits optimization is required for factors such as the intensity of sunlight, photosynthetic pathways, and controllable parameters in engineered systems (e.g., CWMFCs), such as pH, flow rate, COD levels, should be optimized. In order to improve the uptake and commercialization of PhMFC technology, construction and components should be evaluated closely as well, with special attention being paid to electrode materials, their topography, and separation membranes. And finally, the types of phototrophic

organisms and their implementation (e.g., crop rotation schedules and maintenance) will be a central area of focus for future development.

While the field of phototrophic MFCs is rapidly developing, numerous gaps still exist (e.g., type of microbes or substrates, pH, operational procedures like batch mode or continuous mode, design of the device, etc.), requiring enhancement of the wastewater detection and power production capabilities. Thus, multidisciplinary research is needed to study rhizosphere mechanisms between the bacteria, plants (along with rhizodeposition) and electrode environment should be carefully considered for the optimal performance of PhMFCs. To this end, new technology may help probe the nexus between phototrophic organisms and MFCs. One promising direction involves microfluidic lab-on-a-chip systems, which enable growth and real-time monitoring of living organisms such as soil bacteria [177–180], biofilms [181,182], and even plant roots under highly controlled conditions [183–185]. For example, there are an increasing number of studies using microfluidics to study naturally fluorescent photosynthetic bacteria, sometimes termed nanoaquariums. Such studies usually take advantage of pigment autofluorescence and advanced analytical and analysis techniques ranging from deep learning from hyperspectral images and, integrated micro optics have been used for applications including species segregation, optimizing growth conditions [186–189], and studies into interactions with plant roots[185,186]. In parallel, there exists a growing trend in microfluidic MFCs [190], with especially relevant properties such as those which can grow very mature electroactive biofilms that can study device optimal operation conditions [191,192], and the ability to directly visualize the electroactive bacteria [193]. We look forward to these tools, which are being constantly developed thanks to new microfabrication techniques,[194] and applied to other microfluidic biofilm work,[195] being leveraged for detailed studies into the interactions between photosynthetic organisms and their subsystems (e.g., roots) with electrode environments in MFCs.

Finally, we note that there exists a broad spectrum of microbial electrochemical technologies (METs) that may benefit from the inclusion of photosynthetic organisms. These include, but are not limited to: microbial desalination cells (MDCs); microbial electrolysis cells (MECs) which are usually used for hydrogen gas production, microbial electrosynthesis systems (MESs) that are designed to produce soluble organic molecules, such as acetate; and microbial methanogenesis cell (MMC), which produces methane from the cathode [196]. The use of plants

and photosynthetic microbes should be investigated as a way to enhance and diversify the performance of such emerging systems.

## ■ Author contributions

**Jayesh M. Sonawane:** outline generation, original draft preparation, compilation of the sections, table preparations, writing – review and editing. **Ankisha Vijay:** original draft preparation, figure generation; **Tianyang Deng:** original draft preparation; **Prakash Ghosh:** writing – review and editing; **Jesse Greener:** original draft preparation, compilation of sections, figure generation, table preparation, project administration, writing – review and editing.

## ■ Declaration of Competing Interest

The authors declare that they have no known competing financial interests or personal relationships that could have influenced the work reported in this paper.

## References

1    I. Bashir, F. A. Lone, R. A. Bhat, S. A. Mir, Z. A. Dar and S. A. Dar, in *Bioremediation and Biotechnology: Sustainable Approaches to Pollution Degradation*, Springer International Publishing, 2020, pp. 1–26.

2    P. J. van den B. and M. L. Ralf B. Schafer, in *Ecological Impacts of Toxic Chemicals (Open Access)*, Bentham Science Publishers, 2012, pp. 111–137.

3    C. J. Houtman, *J. Integr. Environ. Sci.*, 2010, 7, 271–295.

4    J. M. Sonawane, C. I. Ezugwu and P. C. Ghosh, *ACS Sensors*, 2020, **5**, 2297–2316.

5    R. Lindsey, Climate Change: Atmospheric Carbon Dioxide, https://www.climate.gov/news-features/understanding-climate/climate-change-atmospheric-carbon-dioxide, (accessed 7 September 2020).

6    J. M. Sonawane, S. A. Patil, P. C. Ghosh and S. B. Adeloju, *J. Power Sources*, 2018,

**379**, 103–114.

7    M. Siegert, J. M. Sonawane, C. I. Ezugwu and R. Prasad, in *Nanotechnology in the Life Sciences*, Springer, Cham, 2019, pp. 1–23.

8    A. Vijay, A. Khandelwal, M. Chhabra and T. Vincent, *Chem. Eng. J.*, 2020, **388**, 124157.

9    J. M. Sonawane, R. Mahadevan, A. Pandey and J. Greener, *Heliyon*, 2022, **8**, e12353.

10   H. P. B. R.M. Allen, *Appl. Biochem. Biotechnol*, 1993, **39**, 27–40.

11   A. Vijay, S. Arora, S. Gupta and M. Chhabra, *Bioresour. Technol.*, 2018, **256**, 391–398.

12   J. M. Sonawane, A. Yadav, P. C. Ghosh and S. B. Adeloju, *Biosens. Bioelectron.*, 2017, 90, 558–576.

13   J. M. Sonawane, D. Pant, P. C. Ghosh and S. B. Adeloju, *ACS Appl. Energy Mater.*, 2019, **2**, 1891–1902.

14   C. Corbella and J. Puigagut, *Contrib. to Sci.*, 2015, **11**, 113–120.

15   J. M. Sonawane, A. Gupta and P. C. Ghosh, *Int. J. Hydrogen Energy*, 2013, **38**, 5106–5114.

16   B. E. Logan, B. Hamelers, R. Rozendal, U. Schröder, J. Keller, S. Freguia, P. Aelterman, W. Verstraete and K. Rabaey, *Environ. Sci. Technol.*, 2006, 40, 5181–5192.

17   B. E. Logan, *Microbial Fuel Cells | Wiley*, 2008.

18   A. J. McCormick, P. Bombelli, R. W. Bradley, R. Thorne, T. Wenzel and C. J. Howe, *Energy Environ. Sci.*, 2015, 8, 1092–1109.

19   J. Tschörtner, B. Lai and J. O. Krömer, *Front. Microbiol.*, 2019, 10, 866.

20   S. W. Hogewoning, E. Wientjes, P. Douwstra, G. Trouwborst, W. van Ieperen, R. Croce and J. Harbinson, *Plant Cell*, 2012, **24**, 1921–1935.

21   P. Srivastava, S. Gupta, V. Garaniya, R. Abbassi and A. K. Yadav, *Environ. Chem. Lett.*, 2019, **17**, 1045–1051.

22   P. J. Sarma, B. Malakar and K. Mohanty, *Biomass Convers. Biorefinery*, 2023, 1–14.

23   G. Venkata Subhash, R. Chandra and S. Venkata Mohan, *Bioresour. Technol.*, 2013, **136**, 644–653.

24   R. Sirohi, A. Kumar Pandey, P. Ranganathan, S. Singh, A. Udayan, M. Kumar Awasthi, A. T. Hoang, C. R. Chilakamarry, S. H. Kim and S. J. Sim, *Bioresour. Technol.*, 2022, **349**, 126858.

25   M. Fabris, R. M. Abbriano, M. Pernice, D. L. Sutherland, A. S. Commault, C. C. Hall, L. Labeeuw, J. I. McCauley, U. Kuzhiuparambil, P. Ray, T. Kahlke and P. J. Ralph, *Front. Plant Sci.*, 2020, 11, 279.

26    D. Shevela, L. O. Björn and Govindjee, *Nat. Artif. Photosynth.*, 2013, 13–63.

27    D. P. B. T. B. Strik, R. A. Timmers, M. Helder, K. J. J. Steinbusch, H. V. M. Hamelers and C. J. N. Buisman, *Trends Biotechnol.*, 2011, 29, 41–49.

28    J. M. Lynch and J. M. Whipps, *Plant Soil*, 1990, **129**, 1–10.

29    H. V. M. Hamelers, A. Ter Heijne, T. H. J. A. Sleutels, A. W. Jeremiasse, D. P. B. T. B. Strik and C. J. N. Buisman, *Appl. Microbiol. Biotechnol.*, 2010, 85, 1673–1685.

30    D. P. B. T. B. Strik, H. V. M. Hamelers and C. J. N. Buisman, *Environ. Sci. Technol.*, 2010, **44**, 532–537.

31    J. Dharinee, K. Dhayalini and R. Ranjeet Skanda, in *2022 2nd International Conference on Advances in Electrical, Computing, Communication and Sustainable Technologies, ICAECT 2022*, Institute of Electrical and Electronics Engineers Inc., 2022.

32    F. Y. Lin, Y. Y. Lin, H. T. Li, C. S. Ni, C. I. Liu, C. Y. Guan, C. C. Chang, C. P. Yu, W. S. Chen, T. Y. Liu and H. Y. Chen, *Appl. Energy*, 2022, **325**, 119807.

33    L. De Schamphelaire, A. Cabezas, M. Marzorati, M. W. Friedrich, N. Boon and W. Verstraete, *Appl. Environ. Microbiol.*, 2010, **76**, 2002–2008.

34    K. Takanezawa, K. Nishio, S. Kato, K. Hashimoto and K. Watanabe, *Biosci. Biotechnol. Biochem.*, 2010, **74**, 1271–1273.

35    M. Helder, D. P. B. T. B. Strik, H. V. M. Hamelers, A. J. Kuhn, C. Blok and C. J. N. Buisman, *Bioresour. Technol.*, 2010, **101**, 3541–3547.

36    S. Maddalwar, K. Kumar Nayak, M. Kumar and L. Singh, *Bioresour. Technol.*, 2021, 341, 125772.

37    Y.-Y. Lin, H.-T. Li, H.-Y. Chen and T.-Y. Liu, *ECS Meet. Abstr.*, 2022, **MA2022-01**, 52–52.

38    M. E. Toal, C. Yeomans, K. Killham and A. A. Meharg, *Plant Soil*, 2000, 222, 263–281.

39    L. Gong, M. Abbaszadeh Amirdehi, A. Miled and J. Greener, *Sustain. Energy Fuels*, 2021, **5**, 671–677.

40    R. Nitisoravut and R. Regmi, *Renew. Sustain. Energy Rev.*, 2017, 76, 81–89.

41    H. Li, Y. Tian, Y. Qu, Y. Qiu, J. Liu and Y. Feng, *Sci. Rep.*, 2017, **7**, 1–9.

42    H. P. Bais, T. L. Weir, L. G. Perry, S. Gilroy and J. M. Vivanco, *Annu. Rev. Plant Biol.*, 2006, 57, 233–266.

43    J. M. Lynch, *The Rhizosphere, John Wiley & Sons*, 1990.

44    J. Pausch and Y. Kuzyakov, *J. Plant Nutr. Soil Sci.*, 2011, **174**, 12–19.

45    S. Enríquez, C. M. Duarte and K. Sand-Jensen, *Oecologia*, 1993, 94, 457–471.

46    Y. Kuzyakov, *Soil Biol. Biochem.*, 2010, **42**, 1363–1371.

47    M. Eisenhut, A. Bräutigam, S. Timm, A. Florian, T. Tohge, A. R. Fernie, H. Bauwe and A. P. M. Weber, *Mol. Plant*, 2017, **10**, 47–61.

48    A. K. Sivaram, P. Logeshwaran, S. R. Subashchandrabose, R. Lockington, R. Naidu and M. Megharaj, *Sci. Rep.*, 2018, **8**, 1–10.

49    C. Wang, L. Guo, Y. Li and Z. Wang, *BMC Syst. Biol.*, 2012, **6**, 1–14.

50    D. P. B. T. B. Strik, H. Terlouw, H. V. M. Hamelers and C. J. N. Buisman, *Appl. Microbiol. Biotechnol.*, 2008, **81**, 659–668.

51    B. Chen, W. Cai and A. Garg, *Acta Geotech.*, 2023, 1–14.

52    T. Kuleshova, A. Rao, S. Bhadra, V. K. Garlapati, S. Sharma, A. Kaushik, P. Goswami, T. R. Sreekirshnan and S. Sevda, *Biomass and Bioenergy*, 2022, 167, 106629.

53    Y. Liu, S. Pang, T. Liang, R. Ren and Y. Lv, *Chemosphere*, 2021, **280**, 130776.

54    M. Di Lorenzo, A. R. Thomson, K. Schneider, P. J. Cameron and I. Ieropoulos, *Biosens. Bioelectron.*, 2014, **62**, 182–188.

55    J. Babauta, R. Renslow, Z. Lewandowski and H. Beyenal, *Biofouling*, 2012, 28, 789–812.

56    Y. Jiang, P. Liang, C. Zhang, Y. Bian, X. Yang, X. Huang and P. R. Girguis, *Bioresour. Technol.*, 2015, **190**, 367–372.

57    D. Ayala-Ruiz, A. Castillo Atoche, E. Ruiz-Ibarra, E. Osorio De La Rosa and J. Vázquez Castillo, *Wirel. Commun. Mob. Comput.*, , DOI:10.1155/2019/8986302.

58    E. Sudirjo, P. De Jager, C. J. N. Buisman and D. P. B. T. B. Strik, *Sensors (Switzerland)*, 2019, **19**, 4647.

59    Y. Lu, X. Hu, L. Tang, B. Peng, J. Tang, T. Zeng, XunkuoZhang and Q. Liu, *Chemosphere*, 2022, **302**, 134779.

60    A. C. Sophia and S. Sreeja, *Sustain. Energy Technol. Assessments*, 2017, **21**, 59–66.

61    K. R. S. Pamintuan and K. M. Sanchez, in *IOP Conference Series: Materials Science and Engineering*, 2019, vol. 703, p. 012037.

62    E. Sudirjo, C. J. N. Buisman and D. P. B. T. B. Strik, *Water (Switzerland)*, 2019, **11**, 1810.

63    R. A. Timmers, M. Rothballer, D. P. B. T. B. Strik, M. Engel, S. Schulz, M. Schloter, A. Hartmann, B. Hamelers and C. Buisman, *Appl. Microbiol. Biotechnol.*, 2012, **94**, 537–548.

64    J. Sarkar and S. Bhattacharyya, *Arch. Thermodyn.*, 2012, **33**, 23–40.

65    S. Venkata Mohan, G. Mohanakrishna and P. Chiranjeevi, *Bioresour. Technol.*, 2011, **102**, 7036–7042.

66    N. Habibul, Y. Hu, Y. K. Wang, W. Chen, H. Q. Yu and G. P. Sheng, *Environ. Sci. Technol.*, 2016, **50**, 3882–3889.

67    L. De Schamphelaire, L. Van Den Bossche, S. D. Hai, M. Höfte, N. Boon, K. Rabaey and W. Verstraete, *Environ. Sci. Technol.*, 2008, **42**, 3053–3058.

68    P. Chiranjeevi, G. Mohanakrishna and S. Venkata Mohan, *Bioresour. Technol.*, 2012, **124**, 364–370.

69    A. Kouzuma, T. Kasai, G. Nakagawa, A. Yamamuro, T. Abe and K. Watanabe, *PLoS One*, 2013, **8**, 2–11.

70    J. B. A. Arends, J. Speeckaert, E. Blondeel, J. De Vrieze, P. Boeckx, W. Verstraete, K. Rabaey and N. Boon, *Appl. Microbiol. Biotechnol.*, 2014, **98**, 3205–3217.

71    R. A. Timmers, D. P. B. T. B. Strik, H. V. M. Hamelers and C. J. N. Buisman, *Appl. Microbiol. Biotechnol.*, 2010, **86**, 973–981.

72    O. Guadarrama-Pérez, T. Gutiérrez-Macías, L. García-Sánchez, V. H. Guadarrama-Pérez and E. B. Estrada-Arriaga, *Int. J. Energy Res.*, 2019, 43, 5106–5127.

73    L. Xu, Y. Zhao, L. Doherty, Y. Hu and X. Hao, *Sci. Rep.*, 2016, **6**, 1–9.

74    P. Clauwaert, K. Rabaey, P. Aelterman, L. De Schamphelaire, T. H. Pham, P. Boeckx, N. Boon and W. Verstraete, *Environ. Sci. Technol.*, 2007, **41**, 3354–3360.

75    B. Zhang, Y. Liu, S. Tong, M. Zheng, Y. Zhao, C. Tian, H. Liu and C. Feng, *J. Power Sources*, 2014, **268**, 423–429.

76    A. O. Babatunde, Y. Q. Zhao, R. J. Doyle, S. M. Rackard, J. L. G. Kumar and Y. S. Hu, *Bioresour. Technol.*, 2011, **102**, 5645–5652.

77    Y. Hu, Y. Zhao and A. Rymszewicz, *Sci. Total Environ.*, 2014, **470–471**, 1197–1204.

78    W. et al. Yu, *Sci. Rep.*

79    L. Doherty, Y. Zhao, X. Zhao and W. Wang, *Chem. Eng. J.*, 2015, **266**, 74–81.

80    W. Qu, P. Loke Show, T. Hasunuma and S. H. Ho, *Bioresour. Technol.*, 2020, **305**, 123072.

81    D. Nagarajan, A. Kusmayadi, H. W. Yen, C. Di Dong, D. J. Lee and J. S. Chang, *Bioresour. Technol.*, 2019, 289, 121718.

82    N. S. Malvankar, M. T. Tuominen and D. R. Lovley, *Energy Environ. Sci.*, 2012, **5**, 5790–5797.

83    I. Araneda, N. F. Tapia, K. L. Allende and I. T. Vargas, *Water (Switzerland)*, 2018, **10**, 1–9.

84    C. Sukkasem, S. Xu, S. Park, P. Boonsawang and H. Liu, *Water Res.*, 2008, **42**, 4743–4750.

85    T. Athulya and K. Anitha, *Int. Res. J. Eng. Technol.*, 2020, 1265–1272.

86    R. Piyare, A. L. Murphy, P. Tosato and D. Brunelli, in *Proceedings - 2017 IEEE 42nd Conference on Local Computer Networks Workshops, LCN Workshops 2017*, 2017, pp. 18–25.

87    V. Kiran Kumar, K. Man Mohan, S. P. Manangath and S. Gajalakshmi, *Int. J. Appl. Eng. Res.*, 2018, **13**, 14948–14955.

88    C. Tang, Y. Zhao, C. Kang, Y. Yang, D. Morgan and L. Xu, *Chem. Eng. J.*, 2019, **373**, 150–160.

89    S. Venkata Mohan, S. Srikanth, S. Veer Raghuvulu, G. Mohanakrishna, A. Kiran Kumar and P. N. Sarma, *Bioresour. Technol.*, 2009, **100**, 2240–2246.

90    G. Wang, Y. Guo, J. Cai, H. Wen, Z. Mao, H. Zhang, X. Wang, L. Ma and M. Zhu, *RSC Adv.*, 2019, **9**, 21460–21472.

91    F. Liu, L. Sun, J. Wan, A. Tang, M. Deng and R. Wu, *RSC Adv.*, 2019, **9**, 5384–5393.

92    C. Duvvury, T. C. Holloway, D. Paradis and A. K. Duong, *Time*, 2015, **195**, 4–7.

93    T. L. R. and B. E. L. F. Rezaei, *Biotechnol. Bioeng.,* 2008, **101**, 1163–1169.

94    A. Sharma, S. Gajbhiye, S. Chauhan and M. Chhabra, *Bioresour. Technol.*, 2021, **340**, 125645.

95    Y. Z. and W. W. L. Doherty, X. Zhao, *Ecol. Eng.*, 2015, **79**, 8–14.

96    T. Xie, Z. Jing, J. Hu, P. Yuan, Y. Liu and S. Cao, *Ecol. Eng.*, 2018, **112**, 65–71.

97    I. D. Widharyanti, M. A. Hendrawan and M. Christwardana, *Int. J. Renew. Energy Dev.*, 2020, **10**, 71–78.

98    C. Corbella, M. Hartl, M. Fernandez-gatell and J. Puigagut, *Sci. Total Environ.*, 2019, **660**, 218–226.

99    J. Liu and B. Mattiasson, *Water Res.*, 2002, 36, 3786–3802.

100   Y. Wu, L. Wang, M. Jin, F. Kong, H. Qi and J. Nan, *Bioresour. Technol.*, 2019, **283**, 129–137.

101   L. De Schamphelaire, K. Rabaey, P. Boeckx, N. Boon and W. Verstraete, *Microb. Biotechnol.*, 2008, 1, 446–462.

102   R. G. Burns, *Soil Biol. Biochem.*, 1982, **14**, 423–427.

103   M. Valdez-Hernández, L. N. Acquaroli, J. Vázquez-Castillo, O. González-Pérez, J. C. Heredia-Lozano, A. Castillo-Atoche, L. Sosa-Vargas and E. Osorio-de-la-Rosa, *Energy Sources, Part A Recover. Util. Environ. Eff.*, 2022, **44**, 2715–2729.

104   T. E. Kuleshova, A. G. Ivanova, A. S. Galushko, I. Y. Kruchinina, O. A. Shilova, O. R. Udalova, A. S. Zhestkov, G. G. Panova and N. R. Gall, *Int. J. Hydrogen Energy*, 2022,

**47**, 24297–24309.

105 Y. Zhou, D. Xu, E. Xiao, D. Xu, P. Xu, X. Zhang, Q. Zhou, F. He and Z. Wu, *J. Environ. Sci. (China)*, 2018, **70**, 54–62.

106 Y. Zhao, S. Collum, M. Phelan, T. Goodbody, L. Doherty and Y. Hu, *Chem. Eng. J.*, 2013, **229**, 364–370.

107 L. Doherty, X. Zhao, Y. Zhao and W. Wang, *Ecol. Eng.*, 2015, **79**, 8–14.

108 Z. Fang, H. L. Song, N. Cang and X. N. Li, *Bioresour. Technol.*, 2013, **144**, 165–171.

109 A. K. Yadav, P. Dash, A. Mohanty, R. Abbassi and B. K. Mishra, *Ecol. Eng.*, 2012, **47**, 126–131.

110 D. Wu, L. Yang, L. Gan, Q. Chen, L. Li, X. Chen, X. Wang, L. Guo and A. Miao, *Ecol. Eng.*, 2015, **84**, 624–631.

111 Y. L. Oon, S. A. Ong, L. N. Ho, Y. S. Wong, F. A. Dahalan, Y. S. Oon, H. K. Lehl and W. E. Thung, *Bioresour. Technol.*, 2016, **203**, 190–197.

112 X. Wang, Y. Tian, H. Liu, X. Zhao and S. Peng, *Sci. Total Environ.*, 2019, **653**, 860–871.

113 H. Wu, J. Zhang, H. H. Ngo, W. Guo, Z. Hu, S. Liang, J. Fan and H. Liu, *Bioresour. Technol.*, 2015, 175, 594–601.

114 H. Liu, S. Cheng and B. E. Logan, *Environ. Sci. Technol.*, 2005, **39**, 5488–5493.

115 W. Lan, J. Zhang, Z. Hu, M. Ji, X. Zhang, J. Zhang, F. Li and G. Yao, *Chem. Eng. J.*, 2018, **335**, 209–214.

116 Y. L. Oon, S. A. Ong, L. N. Ho, Y. S. Wong, Y. S. Oon, H. K. Lehl and W. E. Thung, *Bioresour. Technol.*, 2015, **186**, 270–275.

117 Y. L. Oon, S. A. Ong, L. N. Ho, Y. S. Wong, F. A. Dahalan, Y. S. Oon, H. K. Lehl, W. E. Thung and N. Nordin, *Bioresour. Technol.*, 2017, **224**, 265–275.

118 J. Villaseñor, P. Capilla, M. A. Rodrigo, P. Cañizares and F. J. Fernández, *Water Res.*, 2013, **47**, 6731–6738.

119 H. Li, H. L. Song, X. L. Yang, S. Zhang, Y. L. Yang, L. M. Zhang, H. Xu and Y. W. Wang, *Sci. Total Environ.*, 2018, **637**–**638**, 295–305.

120 S. Zhang, H. L. Song, X. L. Yang, K. Y. Yang and X. Y. Wang, *Chemosphere*, 2016, **164**, 113–119.

121 S. Zhang, H. L. Song, X. L. Yang, Y. L. Yang, K. Y. Yang and X. Y. Wang, *RSC Adv.*, 2016, **6**, 95999–96005.

122 M. Kumar and R. Singh, *Environ. Sci. Water Res. Technol.*, 2020, **6**, 795–808.

123 M. Qin, E. A. Hynes, I. M. Abu-Reesh and Z. He, *J. Clean. Prod.*, 2017, **149**, 856–862.

124    S. Puig, M. Serra, A. Vilar-Sanz, M. Cabré, L. Bañeras, J. Colprim and M. D. Balaguer, *Bioresour. Technol.*, 2011, **102**, 4462–4467.

125    L. Xu, B. Wang, X. Liu, W. Yu and Y. Zhao, *Appl. Energy*, 2018, **214**, 83–91.

126    Y. K. Wang, G. P. Sheng, B. J. Shi, W. W. Li and H. Q. Yu, *Sci. Rep.*, 2013, **3**, 1864.

127    D. R. Lovley, *Nat. Rev. Microbiol.*, 2006, 4, 497–508.

128    A. Kouzuma, N. Kaku and K. Watanabe, *Appl. Microbiol. Biotechnol.*, 2014, 98, 9521–9526.

129    G. Wareen, M. Saeed, N. Ilyas, S. Asif, M. Umair, R. Z. Sayyed, S. Alfarraj, W. A Alrasheed and T. H. Awan, *Chemosphere*, 2023, **313**, 137422.

130    D. Bose, A. Bose, S. Mitra, H. Jain and P. Parashar, *Nat. Environ. Pollut. Technol.*, 2018, **17**, 311–314.

131    S. Pandit, B. K. Nayak and D. Das, *Bioresour. Technol.*, 2012, **107**, 97–102.

132    J. G. Ha, S. K. Lee, S. J. Bai, Y. S. Song, Y. K. Kim, Y. M. Shin and J. H. Park, in *2015 Transducers - 2015 18th International Conference on Solid-State Sensors, Actuators and Microsystems, TRANSDUCERS 2015*, 2015, pp. 1929–1932.

133    S. Oh, B. Min and B. E. Logan, *Environ. Sci. Technol.*, 2004, **38**, 4900–4904.

134    K. Schneider, R. J. Thorne and P. J. Cameron, *Philos. Trans. R. Soc. A Math. Phys. Eng. Sci.*, 2016, **374**, 1–22.

135    S. Ahl, P. J. Cameron, J. Liu, W. Knoll, J. Erlebacher and F. Yu, *Plasmonics*, 2008, **3**, 13–20.

136    D. Fleury, *bioRxiv*, 2017, 166793.

137    K. IWAI, D. T. NGUYEN and K. TAGUCHI, *J. Japan Soc. Appl. Electromagn. Mech.*, 2019, **27**, 102–107.

138    L. Gonzalez Olias, P. J. Cameron and M. Di Lorenzo, *Front. Energy Res.*, 2019, **7**, 1–11.

139    F. Ndayisenga, Z. Yu, Y. Yu, C. H. Lay and D. Zhou, *Bioresour. Technol.*, 2018, **270**, 286–293.

140    H. Hadiyanto, M. Christwardana and C. da Costa, *Energy Sources, Part A Recover. Util. Environ. Eff.*, , DOI:10.1080/15567036.2019.1668085.

141    J. Ali, L. Wang, H. Waseem, B. Song, R. Djellabi and G. Pan, *Environ. Pollut.*, 2020, **266**, 115373.

142    C. Xu, K. Poon, M. M. F. Choi and R. Wang, *Environ. Sci. Pollut. Res.*, 2015, **22**, 15621–15635.

143    A. J. McCormick, P. Bombelli, A. M. Scott, A. J. Philips, A. G. Smith, A. C. Fisher and

C. J. Howe, *Energy Environ. Sci.*, 2011, **4**, 4699–4709.

144 Y. Zou, J. Pisciotta and I. V. Baskakov, *Bioelectrochemistry*, 2010, **79**, 50–56.

145 K. Nishio, K. Hashimoto and K. Watanabe, *Appl. Microbiol. Biotechnol.*, 2010, **86**, 957–964.

146 L. Xiao, E. B. Young, J. A. Berges and Z. He, *Environ. Sci. Technol.*, 2012, **46**, 11459–11466.

147 A. Sharma and M. Chhabra, *Bioresour. Technol.*, 2021, **338**, 125499.

148 X. Wang, Y. Feng, J. Liu, H. Lee, C. Li, N. Li and N. Ren, *Biosens. Bioelectron.*, 2010, **25**, 2639–2643.

149 M. E. Elshobary, H. M. Zabed, J. Yun, G. Zhang and X. Qi, *Int. J. Hydrogen Energy*, 2021, **46**, 3135–3159.

150 L. Gouveia, C. Neves, D. Sebastião, B. P. Nobre and C. T. Matos, *Bioresour. Technol.*, 2014, **154**, 171–177.

151 S. Das, R. Raj, S. Das and M. M. Ghangrekar, *Environ. Sci. Pollut. Res.*, 2022, 1, 1–18.

152 R. Jiang and D. Chu, *Electrochem. Solid-State Lett.*, , DOI:10.1149/1.1480136.

153 S. C. Popat, D. Ki, B. E. Rittmann and C. I. Torres, *ChemSusChem*, 2012, **5**, 1071–1079.

154 L. Zhuang, S. Zhou, Y. Li and Y. Yuan, *Bioresour. Technol.*, 2010, **101**, 3514–3519.

155 T. Liu, L. Rao, Y. Yuan and L. Zhuang, *Sci. World J.*, , DOI:10.1155/2015/864568.

156 S. Angioni, L. Millia, P. Mustarelli, E. Doria, M. E. Temporiti, B. Mannucci, F. Corana and E. Quartarone, *Heliyon*, 2018, **4**, e00560.

157 S. Angioni, L. Millia, G. Bruni, D. Ravelli, P. Mustarelli and E. Quartarone, *J. Power Sources*, 2017, **348**, 57–65.

158 B. Neethu, V. Tholia and M. M. Ghangrekar, *Process Biochem.*, 2020, **95**, 99–107.

159 W. Zhao, T. Chen, Q. Zhang, W. Peng and J. Xie, *Huanjing Kexue Xuebao/Acta Sci. Circumstantiae*, 2014, **34**, 2754–2758.

160 C. Santoro, C. Arbizzani, B. Erable and I. Ieropoulos, *J. Power Sources*, 2017, **356**, 225–244.

161 J. Chouler, M. D. Monti, W. J. Morgan, P. J. Cameron and M. Di Lorenzo, *Electrochim. Acta*, 2019, **309**, 392–401.

162 Z. Yongjin, J. Pisciotta, R. B. Billmyre and I. V. Baskakov, *Biotechnol. Bioeng.*, 2009, **104**, 939–946.

163 M. Zhou, H. He, T. Jin and H. Wang, *J. Power Sources*, 2012, **214**, 216–219.

164 R. Kakarla and B. Min, *Int. J. Hydrogen Energy*, 2014, **39**, 10275–10283.

165 D. Bin Wang, T. S. Song, T. Guo, Q. Zeng and J. Xie, *Int. J. Hydrogen Energy*, 2014,

**39**, 13224–13230.

166    J. Ma, Z. Wang, J. Zhang, T. D. Waite and Z. Wu, *Water Res.*, 2017, **108**, 356–364.

167    A. Khandelwal, A. Vijay, A. Dixit and M. Chhabra, *Bioresour. Technol.*, 2018, **247**, 520–527.

168    E. Bazdar, R. Roshandel, S. Yaghmaei and M. M. Mardanpour, *Bioresour. Technol.*, 2018, **261**, 350–360.

169    J. Lobato, A. González del Campo, F. J. Fernández, P. Cañizares and M. A. Rodrigo, *Appl. Energy*, 2013, **110**, 220–226.

170    W. Logroño, M. Pérez, G. Urquizo, A. Kadier, M. Echeverría, C. Recalde and G. Rákhely, *Chemosphere*, 2017, **176**, 378–388.

171    G. Li, H. Chang, Y. Zou, J. Yue, Y. Zheng, H. Feng, H. Wu, W. Wu, J. Lou, X. Qi and X. Zhang, *Environ. Chem. Lett.*, 2021, **19**, 3531–3537.

172    Y. Zhang, Y. Zhao and M. Zhou, *Environ. Sci. Pollut. Res.*, 2019, **26**, 6182–6190.

173    C. W. Lin, L. K. Alfanti, Y. S. Cheng and S. H. Liu, *Desalination*, 2022, **542**, 116079.

174    S. Liu, Z. Wang, X. Feng and S. H. Pyo, *Environ. Res.*, 2023, **216**, 114625.

175    A. Mishra and M. Chhabra, *Bioresour. Technol. Reports*, 2022, **19**, 101199.

176    C. Corbella, J. Puigagut and M. Garfí, *Sci. Total Environ.*, 2017, **584–585**, 355–362.

177    P. M. Mafla-Endara, C. Arellano-Caicedo, K. Aleklett, M. Pucetaite, P. Ohlsson and E. C. Hammer, *Commun. Biol.*, 2021, **4**, 1–12.

178    H. Dai, Y. Zhuang, E. Stirling, N. Liu and B. Ma, *Soil Ecol. Lett.*, 2023, 5, 21–37.

179    R. Rusconi, M. Garren and R. Stocker, *Annu. Rev. Biophys.*, 2014, **43**, 65–91.

180    C. E. Stanley, G. Grossmann, X. CasadevallI Solvas and A. J. DeMello, *Lab Chip*, 2016, **16**, 228–241.

181    S. Subramanian, R. C. Huiszoon, S. Chu, W. E. Bentley and R. Ghodssi, *Biofilm*, 2020, 2, 100015.

182    M. Pousti, M. P. Zarabadi, M. Abbaszadeh Amirdehi, F. Paquet-Mercier and J. Greener, *Analyst*, 2019, 144, 68–86.

183    A. Sanati Nezhad, *Lab Chip*, 2014, **14**, 3262–3274.

184    L. Verhage, *Plant J.*, 2021, 108, 301–302.

185    M. Guichard, E. Bertran Garcia de Olalla, C. E. Stanley and G. Grossmann, in *Methods in Cell Biology*, Academic Press, 2020, vol. 160, pp. 381–404.

186    S. C. C. Shih, N. S. Mufti, M. D. Chamberlain, J. Kim and A. R. Wheeler, *Energy Environ. Sci.*, 2014, **7**, 2366–2375.

187    P. Bodénès, H. Y. Wang, T. H. Lee, H. Y. Chen and C. Y. Wang, *Biotechnol. Biofuels*,

2019, **12**, 1–25.

188    Y. Hanada, K. Sugioka, I. Shihira-Ishikawa, H. Kawano, A. Miyawaki and K. Midorikawa, *Lab Chip*, 2011, **11**, 2109–2115.

189    T. Deng, D. DePaoli, L. Bégin, N. Jia, L. T. De Oliveira, D. C. Coté, W. F. Vincent and J. Greener, *Anal. Chem.*, 2021, **93**, 8764–8773.

190    P. Parkhey and R. Sahu, *Int. J. Hydrogen Energy*, 2021, **46**, 3105–3123; (b) M.A. Amirdehi, S. Saem, M.P. Zarabadi, J.M. Moran-Mirabal, J. Greener, Advanced Materials Interfaces, 2018, 1800290.

191    (a) M. A. Amirdehi, N. Khodaparastasgarabad, H. Landari, M. P. Zarabadi, A. Miled and J. Greener, *ChemElectroChem*, 2020, **7**, 2227–2235 (b) M. A. Amirdehi, L. Gong, N. Khodaparastasgarabad, J. M. Sonawane, B. E. Logan and J. Greener, *Electrochim. Acta*, 2022, 139771.

192    (a) M. P. Zarabadi, M. Couture, S. J. Charette and J. Greener, ChemElectroChem, 2019, **6**, 2715-2718; (b) M. P. Zarabadi, F. o. Paquet-Mercier, S. J. Charette and J. Greener, Langmuir, 2017, **33**, 2041-2049 (c) M. P. Zarabadi, S. J. Charette and J. Greener, Sustainable Energy & Fuels, 2019, **3**, 2211-2217

193    D. Ye, P. Zhang, J. Li, X. Zhu, R. Chen and Q. Liao, Int. J. Hydrogen Energy, 2021, **46**, 14651–14658.

194    (a) G. Wegner, N. Allard, A. Al Shboul, M. Auger, et al. Functional materials: For energy, sustainable development and biomedical sciences, Walter de Gruyter GmbH & Co KG, Chaptier 14, 375-410; (b) J. Greener, W. Li, J. Ren, D. Voicu, V. Pakharenko, T. Tang, E. Kumacheva, *Lab Chip*, 2010, **10**, 522–524; (c) L. Hof, X. Guo , M. Seo, R. Wüthrich, J. Greener, *Micromachines*, 2017, **8**, 29; (d) M. Debono, D. Voicu, M. Pousti, M. Safdar, R. Young, E. Kumacheva, J. Greener, *Sensors*, 2016, **16**(12), 2023; A. Kara, A. Reitz, J. Mathault, S. Mehou-Loko, M.A. Amirdehi, A. Miled, J. Greener, *Lab Chip*, 2016, **16**, 1081-1087.

195    (a) F. Paquet-Mercier, M. Parvinzadeh Gashti, J Bellevance, S. Mohammad Taghavi, J. Greener, *Lab Chip*, 2016, **16**, 4710-4717; (b) J. Greener, M. Parvinzadeh Gashti, A. Eslami, M. P. Zarabadi, S. M. Taghavi, *Biomicrofluidics*, 2016, **10**, 064107; (c) J. Greener, W. Harvey, C. Gagné-Thivierge, S. Fakhari, S. M. Taghavi, J. Barbeau, S. Charette, *Physics of Fluids* 2022, **34**, 021902, 1-10; (d) M. Parvinzadeh Gashti, J. Bellavance, O. Kroukamp, G. Wolfaardt, S. M. Taghavi, J. Greener, *Biomicrofluidics*, 2015, **9**, 041101; (e) M. Parvinzadeh Gashti, J. Asselin, J. Barbeau, D. Boudreau, J. Greener, *Lab Chip*, 2016, **16**, 1412-1419; (f) F. Asayesh, M. P. Zarabadi, N. Babaei

Aznaveha and J. Greener, *Anal Methods*, 2018, **10**, 4579 - 4587.

196    B. E. Logan, M. J. Wallack, K.-Y. Kim, W. He, Y. Feng, P. E. Saikaly, *Environ. Sci. Technol. Lett.*, 2015, 2, 206−214.